



Winter wet-dry weather patterns driving atmospheric rivers and Santa Ana winds provide evidence for increasing wildfire hazard in California

Kristen Guirguis¹ · Alexander Gershunov¹ · Benjamin Hatchett² · Tamara Shulgina¹ · Michael J. DeFlorio¹ · Aneesh C. Subramanian³ · Janin Guzman-Morales¹ · Rosana Aguilera¹ · Rachel Clemesha¹ · Thomas W. Corringtonham¹ · Luca Delle Monache¹ · David Reynolds³ · Alex Tardy⁴ · Ivory Small⁴ · F. Martin Ralph¹

Received: 7 September 2021 / Accepted: 25 May 2022 / Published online: 17 July 2022
© The Author(s) 2022

Abstract

Floods caused by atmospheric rivers and wildfires fanned by Santa Ana winds are common occurrences in California with devastating societal impacts. In this work, we show that winter weather variability in California, including the occurrence of extreme and impactful events, is linked to four atmospheric circulation regimes over the North Pacific Ocean previously named and identified as the “NP4 modes”. These modes come in and out of phase with each other during the season, resulting in distinct weather patterns that recur throughout the historical record. Some phase combinations favor atmospheric river landfalls and extreme daily or multi-day precipitation, while other phase combinations favor anomalously hot weather and drying Santa Ana wind conditions over Southern California. This historical perspective of atmospheric circulation and impacts over 70 years reveals that weather patterns are changing in a way that enhances wildfire hazard in California, while the frequency of weather patterns linked to historical floods is not diminishing. These changes highlight the rising hazards of cascading weather extremes in California’s present and future.

1 Introduction

Extreme winter weather variability in California is largely driven by the interplay between onshore landfalling atmospheric rivers and offshore downslope winds that bring desiccating desert conditions often associated with coastal heat and sometimes spreading wildfire. Atmospheric rivers (ARs) are narrow filaments of concentrated atmospheric water vapor that can bring extreme orographically-enhanced precipitation during fall and winter. While critical for California’s water resources, ARs are also the major cause of historical riverine floods (Ralph et al. 2006, 2011; Corringtonham et al. 2019). Downslope Santa Ana winds (SAWs)

are characteristically hot, dry, offshore winds that bring fire weather to coastal and inland Southern California (Abatzoglou et al. 2021). SAWs are linked with Southern California’s most destructive wildfires (Westerling et al. 2004; Moritz et al. 2010; Kolden and Abatzoglou 2018; Gershunov et al. 2021). Typically, the SAW season begins in fall and peaks in December (Guzman Morales et al. 2016). The timing of offshore winds relative to ARs is an important factor for hazardous wildfires in California, where the risk of a destructive wildfire is enhanced if a strong offshore wind event such as a SAW—or their northern California counterpart the Diablo wind (Abatzoglou et al. 2021)—occurs before the first fall or winter rains when fuel moisture is at its climatological minimum. ARs and downslope winds are driven by certain recurring weather patterns over and offshore of western North America that favor onshore or offshore flow over California, respectively (e.g. Ralph et al. 2004; Neiman et al. 2008; Guirguis et al. 2018; Hughes and Hall 2010; Abatzoglou et al. 2013; Guzman Morales et al. 2016). Both flow regimes have important implications for California’s land and water resources and pose hazards to life and property.

✉ Kristen Guirguis
kguirguis@ucsd.edu

¹ Scripps Institution of Oceanography, University of California, San Diego, 9500 Gilman Drive, 0224, La Jolla, CA 92093, USA

² Desert Research Institute, Reno, NV, USA

³ University of Colorado Boulder, Boulder, CO, USA

⁴ U.S. National Weather Service, San Diego, CA, USA

Previous studies have demonstrated the importance of certain atmospheric circulation patterns in driving AR landfalls over California and western North America. AR landfalls are often associated with a ridge situated over/near Alaska ($\sim 160^{\circ}\text{W}$) with a trough to the southeast and a strong pressure gradient that channels marine moisture toward the coast (e.g. Weaver 1962; Strobin and Reynolds 1995; Ralph et al. 2004; Neiman et al. 2008; Guirguis et al. 2018, 2019, 2020a). The position, strength, and orientation of these circulation features relative to coastal topography modulate the landfall location as well as the amount and spatial distribution of moisture transport and precipitation (Neiman et al. 2008; Mundhenk et al. 2016; Swales et al. 2016; Hecht and Cordeira 2017; Hu et al. 2017; Guirguis et al. 2019). ARs have also been linked to extratropical cyclones and closed low pressure systems (Oakley et al. 2017; Zhang et al. 2019).

SAWs are associated with anomalous surface high pressure centered over the interior Great Basin driving anticyclonic flow through complex terrain bringing strong, dry easterly/hortheasterly downslope winds to Southern California (Hughes and Hall 2010; Abatzoglou et al. 2013; Guzman Morales et al. 2016). These winds warm by adiabatic compression as air flows from above the elevated Great Basin, ascends over the 3000 m high Transverse and Peninsular Ranges or is funneled through mountain passes and ultimately descends down to sea level. This warming leads to coastal heat waves in the fall, winter and spring (Gershunov et al. 2021). The associated hot, dry, and windy conditions during periods of low fuel moisture in fire-prone ecosystems creates substantial fire hazard in wildland and adjacent communities. Harmful health impacts associated with SAW-driven heat waves (Schwarz et al. 2020) and wildfire smoke (Aguilera et al. 2020, 2021) have also been reported. While all SAWs warm adiabatically, they do not always produce heat waves at the coast. Hot and cold SAWs result from distinctly different synoptic dynamics and Great Basin land surface conditions (Gershunov et al. 2021). All SAWs involve a surface high pressure over the northeastern Great Basin, which develops in association with a blocking high aloft in the case of hot SAWs and with Rossby wave breaking in the wake of transient cold frontal cyclones in the case of cold SAWs; the latter are also associated with anomalous positive snow cover in the Great Basin (Gershunov et al. 2021). Southern California wildfires are preferentially spread by hot SAWs (Gershunov et al. 2021).

Typically, the interplay between ARs, SAWs, extreme precipitation, and wildfires is thought of as a situation where one extreme (ARs) is the remedy or prevention of the other extreme (wildfires). However, when ARs occur following wildfires, they can cause deadly and damaging post-fire debris flows or flash flooding over burn scars if short-duration, high intensity rainfall occurs (Oakley et al. 2017, 2018), compounding the original impacts of

wildfire. Here, we show that ARs and SAWs are more closely linked than previously discovered through interacting synoptic-scale atmospheric circulation regimes. Specifically, we demonstrate how four key circulation regimes over the North Pacific Ocean (“North Pacific Modes” or “NP4 modes”), identified and described in previous work (Guirguis et al. 2020a, hereinafter GGR’20), interact on daily timescales to produce recurring, regionally-important weather patterns responsible for impactful weather in California and along the West Coast. These four circulation regimes (shown in Fig. 1a) are known as the Baja-Pacific (BP), Alaskan-Pacific (AP) Canadian-Pacific (CP), and Offshore-California (OC) modes. The NP4 modes share characteristics with established, well-known teleconnections identified in previous work. For example, the Alaskan-Pacific and Canadian-Pacific modes are related to the well-known East Pacific Oscillation (EPO) and Pacific North American (PNA) Pattern, respectively (GGR’20), which were first identified in Barnston and Livezey (1987). Other studies aiming to identify circulation regimes over this region have found similar patterns (e.g. Straus et al. 2007; Amini and Strauss 2019; Gibson et al. 2020).

The NP4 modes represent four winter teleconnections identified by the preferred position of atmospheric ridges and troughs over the North Pacific Ocean and along the West Coast. As these modes fluctuate, they can shift in- or out-of-phase with each other on a given day, and seasonally they exhibit a strong tendency to persist in one phase over the other (GGR’20). The joint phase combination of the NP4 modes has been shown to strongly modulate coastal water vapor transport, AR landfalls, and California precipitation, and has been linked to historical floods (GGR’20). In this study, we extend the relevance of the NP4 mode interactions to other types of extreme weather events and their consequences, including SAWs and historical wildfires, and show how these interactions produce distinct weather patterns that recur throughout the historical record. We focus mostly on the interplay between ARs and SAWs (and associated floods and wildfires), but also discuss heat waves, cold extremes, and snowpack accumulation.

We first classify and describe the dominant, recurring weather patterns impacting California and the western US during the extended winter season (Nov–Feb; Sect. 3). We then identify those weather patterns associated with ARs, extreme precipitation, and historical floods (Sect. 4) and those associated with Santa Ana winds and wildfires (Sect. 5). In Sect. 6, we diagnose and explain observed trends in weather pattern frequency and discuss the implications for wildfire hazard and water resources. Finally, we provide a summary and discuss the implications for resource and emergency management, subseasonal-to-seasonal (S2S) forecasting, and climate change (Sect. 7).

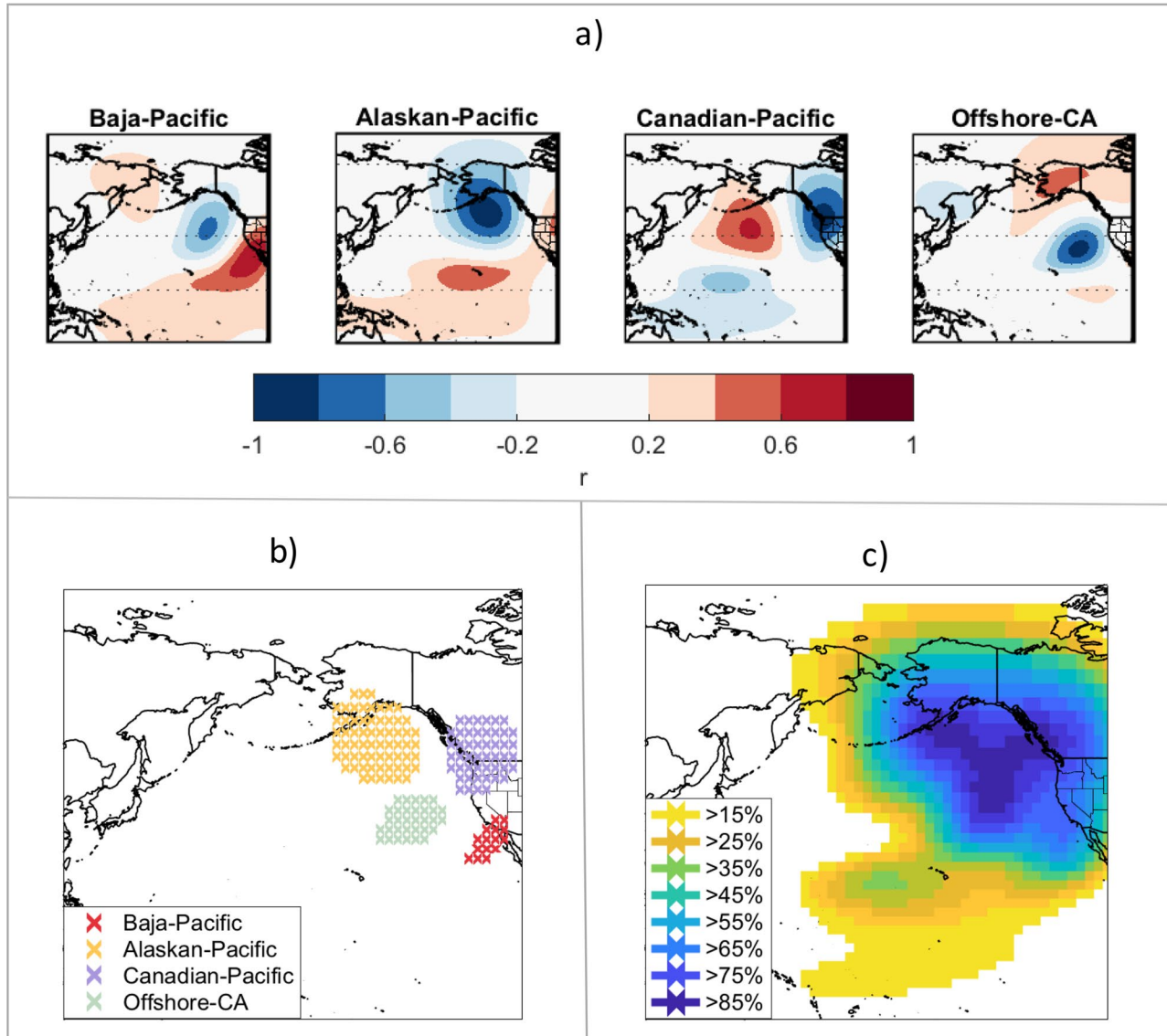


Fig. 1 **a** The four North Pacific atmospheric teleconnection patterns (NP4 modes) defined and described in GGR'20 shown here in the phase most associated with wet conditions over California (defined as the positive phase as in GGR'20). The color scale gives the temporal correlation (r) between each teleconnection pattern and the standard-

ized Z500 anomalies at each grid cell (**b**) locations where more than 50% of Z500 variance is explained by one of the NP4 modes using linear regression with $r^2 > 0.5$, **c** total Z500 variance explained by the joint NP4 modes using multiple linear regression. Figures (**a**, **c**) are adapted from GGR'20

2 Data and methods

2.1 Time period of study

Our time period of study spans 1949–2021. However, some variables have shorter records due to data availability. The season of focus is extended winter (November–February; hereafter winter) to coincide with the NP4 dataset (described in Sect. 2.8), and which is also the part of the season most active with respect to both AR activity

and SAW activity in California (Gershunov et al. 2017, and Guzman-Morales and Gershunov 2019, respectively). We note the focus on extended winter omits many of the most destructive SAW events occurring in the early fall. However, winter SAWs do pose substantial fire hazard when they occur before the first seasonal rain or during drought years. For example, the Thomas Fire, fanned by successive SAWs, burned through most of December of 2017 and into January 2018 to become (for a time) the biggest wildfire in California history.

2.2 Atmospheric variables

Daily 500 mb geopotential height (Z500) and wind fields for the period spanning Nov–Feb 1949–2021 are from NCEP/NCAR 2.5° global reanalysis (Kalnay et al. 1996). Daily anomalies were calculated relative to the annual/semiannual seasonal cycle fit using least squares regression.

2.3 Atmospheric river detection and AR intensity scale

The SIO-R1 catalog of Gershunov et al. (2017) is used to identify landfalling ARs along the coast of western North America. The detection method uses threshold criteria for 6-hourly integrated water vapor ($IWV > 15 \text{ mm}$) and integrated vapor transport ($IVT > 250 \text{ kg m}^{-1} \text{ s}^{-1}$) to identify elongated objects of high moisture content that intersect the coast. The AR scale of Ralph et al. (2019) is used to categorize the magnitude of storms. This 5-scale classification is based on IVT magnitude and duration where the scale 1–5 describes ARs as weak, moderate, strong, extreme, and exceptional, respectively. AR scales 1–2 are mostly beneficial providing needed precipitation without damage, whereas AR scales 4–5 are mostly hazardous with peak IVT in the range of 750 to more than $1250 \text{ kg m}^{-1} \text{ s}^{-1}$. Flood damages in the western U.S. increase exponentially with the AR scale (Corringham et al. 2019). The SIO-RI AR catalog is available at <https://weclima.ucsd.edu/data-products/>.

2.4 Santa Ana winds

Historical SAW events are identified using the daily Santa Ana Winds Regional Index (SAWRI) of Guzman Morales et al. 2016. This data product is based on 65 years of hourly data from the dynamically downscaled CaRD10 dataset (Kanamitsu and Kanamaru 2007) and validated against station observations. This study uses the updated daily version of Guzman-Morales and Gershunov (2019). The SAWRI methodology identifies SAWs at each grid cell if certain surface wind conditions are met (wind speeds exceeding the local 75th percentile with a northerly to easterly direction). Then, a regional SAW index is provided by averaging local SAW conditions over a region of concurrent northeasterly strong winds that expands from the leeside of the transversal and peninsular mountain ranges to the low-elevation coastal region of Southern California. The SAWRI dataset is available at <https://weclima.ucsd.edu/data-products/>. In this study we define moderate (extreme) SAWs as those exceeding the 50th (90th) percentile in the SAWRI record.

2.5 Historical temperature and precipitation

Daily precipitation and maximum temperature (Tmax) data are from Livneh et al. (2013, 2015), which is a gridded data product available at a 1/16° spatial resolution over the period 1950–2015 (available at <https://climatedataguide.ucar.edu/climate-data>). The source data are from approximately 20,000 stations in the Global Historical Climatology Network (GHCN). Extreme precipitation is defined as daily accumulation above the 95th percentile. Heat waves (cold extremes) are defined following Gershunov and Guirguis (2012) as daily temperatures persisting for at least one day above the 95th (below the 5th) percentile after removing the seasonal cycle.

2.6 Sierra Nevada snowpack

We use monthly snow water equivalent data from a single snow course in the Northern Sierra Nevada. Specifically, we selected Donner Summit (39.3° N , -120.3° W , elevation 2100 m, station ID 20K10) from the Natural Resources Conservation Service (<https://wcc.sc.egov.usda.gov/nwcc/rgrpt?report=snowcourse&state=CA>). This location sits at the intersection of three key headwater regions (Yuba, Truckee, and American Rivers) involved in managing California and Nevada water resources. The Donner Summit snow course has a long (1913–2021) and complete record.

2.7 Wildfire

Wildfire information is from the California Fire Protection's Fire and Resource Assessment Program (FRAP) fire perimeters database (<https://frap.fire.ca.gov/frap-projects/fire-perimeters/>). We focus on fire start dates for historical wildfires with burn sizes exceeding 1000 acres in the Southern California (SoCal) counties of Santa Barbara, Ventura, Los Angeles, Orange, Riverside, San Bernardino, and San Diego. Our sample includes 76 wildfires spanning 1949–2018, with most occurring in November ($n=40$) or December ($n=21$). As mentioned above, most wildfires in California occur in October, which is outside of our extended winter focus season. However, the wildfire season can and does extend into winter during drought years or when delayed rains extend dry vegetation into the peak of SAW season.

2.8 North Pacific atmospheric circulation regimes

We use daily amplitudes of four North Pacific atmospheric circulation regimes (NP4 modes), which were identified and shown to be essential drivers of vapor transport and AR activity along the coast of western North America by Guirguis et al. (2018, hereinafter GGR'18) and GGR'20. These four modes are named according to their geographic

centers of action: Baja-Pacific (BP), Alaskan-Pacific (AP), Canadian-Pacific (CP), and Offshore-California (OC) modes. The NP4 modes were identified using rotated Empirical Orthogonal Function (EOF) analysis applied to Z500 anomaly fields over a large domain spanning the northern Pacific Ocean and western North America. While the NP4 modes are not the most important in terms of field variance (i.e., they correspond to higher-order rotated principal components), they were found to be the most important modes for coastal IVT, AR landfalls, and extreme precipitation in California (GGR'18, GGR'20). The EOF loading patterns (maps) associated with the positive phase of each mode are shown in Fig. 1a. The portion of the domain where these modes are most influential is shown in Fig. 1b, c. Specifically, Fig. 1b shows the locations where one of the four modes is by itself responsible for more than 50% of the Z500 variance. Figure 1c shows the collective influence of the four modes, where we see that together these modes explain 25–90% variance in the portion of the domain most relevant for west coast weather. The NP4 dataset used in this study is described in Guirguis et al. (2020b) and is available at <https://doi.org/10.6075/J0154FJJ>.

2.9 Weather regime classification

Daily weather regimes are classified based on the joint phase combination of the NP4 modes. As the NP4 modes oscillate over the North Pacific, their daily interactions determine the position and strength of ridges and troughs along the coast of western North America. Unique NP4 phase combinations result in distinct weather patterns that drive extreme weather in California (GGR'18 GGR'20). On a given day, each of the four NP4 modes can be positive or negative, which yields 16 possible phase combinations, and 16 corresponding weather regimes (introduced and described in Sect. 3).

We use the terminology “weather pattern” and “weather regime” somewhat interchangeably. “Weather pattern” is taken to mean the Z500 anomaly field itself while “weather regime” refers to the classification of that pattern. A catalog of historical weather regimes observed over 1949–2017 is developed as an accompaniment to this publication (Guirguis et al. 2022) and is available from the UC San Diego Library Digital Collections at <https://doi.org/10.6075/J089161B>

3 Winter weather patterns impacting the West Coast

Figure 2 shows Z500 anomaly patterns associated with the sixteen different phase combinations of the NP4 modes, which are used to define winter weather regimes (WR) impacting the West Coast. We first provide examples of how the NP4 modes interact to create distinct weather patterns

(Sect. 3.1) and then provide an overview of circulation characteristics and impacts associated with each weather regime (Sect. 3.2).

3.1 How the NP4 modes interact to produce distinct weather patterns

Examples of how the NP4 modes interact to produce distinct weather patterns are provided in Figs. 3 and 4 for 2016–2017 (a wet year) and 2020–2021 (a dry year), respectively (e.g. Abatzoglou et al. 2017, <https://wrcc.dri.edu/wwdt/>).

Figure 3 shows the daily NP4 amplitudes (Fig. 3a) and daily interactions (Fig. 3b) for water year 2016–2017 (WY2017). We highlight three events (December 7–16, January 3–11, and February 1–8) when the NP4 modes exhibited the same joint phase configuration (labeled E1, E2, and E3; Fig. 3). Specifically, during these three events the BP mode was positive (which favors a ridge over Baja California, c.f. Fig. 1a), the AP mode was negative (favoring high pressure over Alaska), and the OC and CP modes were positive (favoring low pressure over western Canada and offshore from California, respectively). This mode configuration results in the atmospheric circulation and IVT patterns shown in Fig. 3c, d, respectively. This type of pattern (classified as WR10, see Fig. 2) is associated with strong onshore flow, AR landfalls, and wet conditions over Central and Southern California with heavy precipitation over the Sierra Nevada. In this example, the February 1–8 event highlights the Oroville Dam crisis (Vahedifard et al. 2017) that resulted in the evacuation of over 180,000 people due to spillway damage from extreme runoff during intense and prolonged AR precipitation with high snow levels causing rain-on-snow. These three events also produced flooding on the leeside of the Sierra Nevada (Henn et al. 2020; Sterle et al. 2019).

The second example is for WY 2021 (Fig. 4). Here we highlight three different events (November 1–4, November 27–December 8, and January 9–17) sharing a common NP4 phase combination. For these events (labeled E4–E6), the BP and AP modes were positive (favoring a ridge over Baja California and a trough over Alaska, respectively, c.f. Fig. 1a) and the CP and OC modes were negative (favoring high pressure over western Canada and offshore California, respectively). This combination results in the atmospheric circulation (Fig. 4c) and IVT patterns (Fig. 4d), featuring anomalous onshore flow over British Columbia/Pacific Northwest and offshore flow over Southern California. This pattern of circulation (classified as WR5, see Fig. 2) is associated with ARs in the northern latitudes (Pacific Northwest/British Columbia) and SAW conditions over Southern California. The two longer events (E5 and E6) prompted Red Flag Warnings in Southern California along with large-scale public safety power shutoffs initiated by electric companies

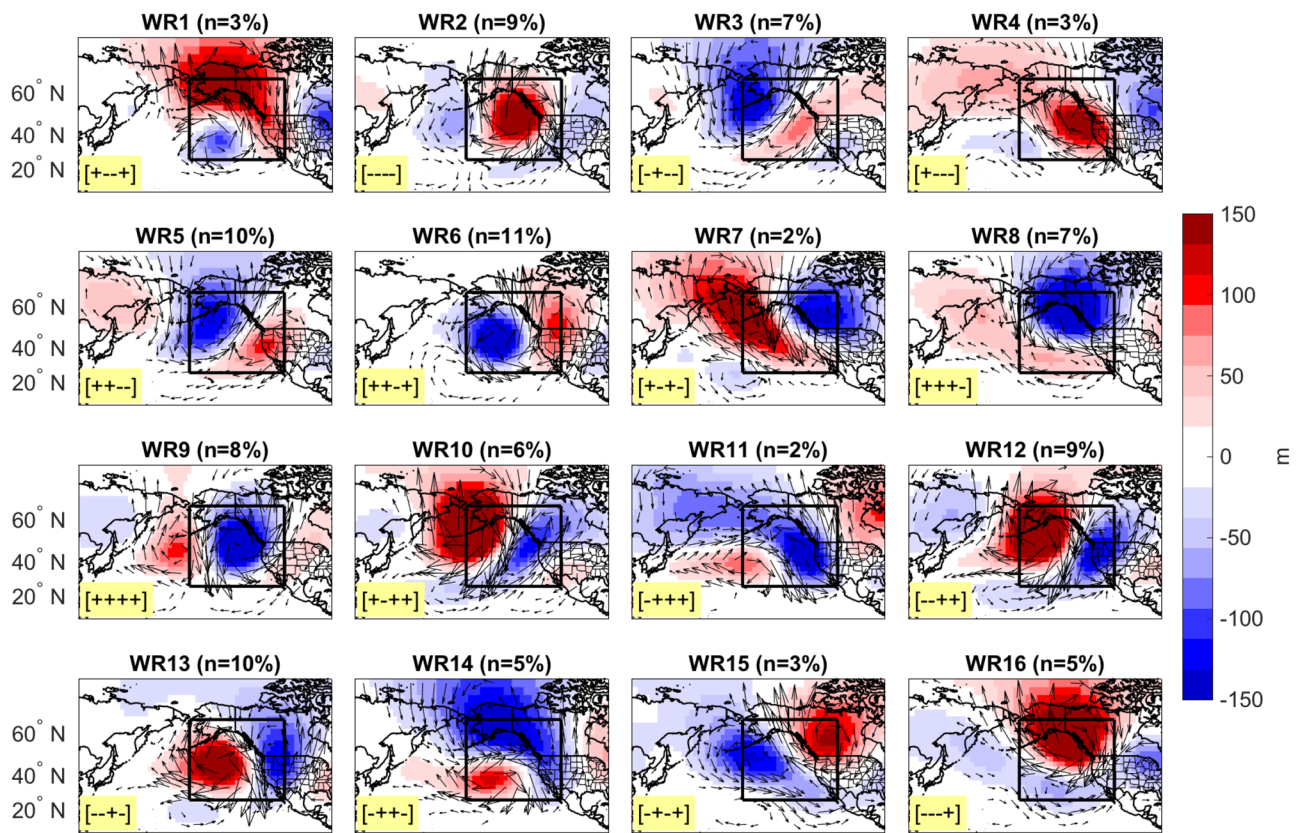


Fig. 2 Composites of 500 mb geopotential height anomalies for the sixteen recurring winter weather patterns impacting West Coast. The sample size of each weather regime (n) is given in the title as a percentage of total days in the 1949–2017 record. The highlighted ± in the lower left corner gives the phase of the NP4 modes in the following order: [BP, AP, CP, OC]

percentage of total days in the 1949–2017 record. The highlighted ± in the lower left corner gives the phase of the NP4 modes in the following order: [BP, AP, CP, OC]

to prevent accidental ignitions by utility equipment (Murphy 2021; Chediak and Sullivan 2021).

Within a weather regime class, defined by the joint NP4 phase, the mode amplitudes can vary from nearly zero to very extreme. These amplitude differences cause variability in the orientation and strength of influential circulation anomaly features, which directly affects the location and magnitude of associated impacts. It follows that the impacts associated with each weather regime are considered in a probabilistic sense to account for this variability.

3.2 Impacts and circulation characteristics associated with each weather regime

Impacts associated with each weather regime are shown in Fig. 5 for AR landfall probabilities (a), precipitation anomalies (b), probability of extreme precipitation (c), and percent of total historical precipitation (d). Additional impacts are shown in Fig. 6 for SAW probabilities (a), temperature anomalies (b), heat wave probabilities (c), and cold extreme probabilities (d). The specific NP4 phase combination associated with each weather regime is shown in Figure S1 and is also displayed as highlighted text in the lower left of each

map in Fig. 2. For all weather regimes shown in Fig. 2, the salient ridge/trough features are well represented by the vast majority of days within each weather regime class. For example, Figure S2 shows the percent agreement among days within each sample in the sign of the Z500 anomaly, which reaches 94–100% for ridge/trough positions at the point of maximum overlap.

Weather regimes 1–6 feature a strong ridge positioned over/offshore western North America (Fig. 2), creating atmospheric blocking conditions that produce dry weather over much of the western US, especially California (Fig. 5b–d). Offshore flow occurs over Southern California along the eastern boundary of the ridge, bringing elevated chances of SAW conditions (Fig. 6a). Four of these patterns (WR1, WR4, WR5 and WR6) favor warm temperatures, with an elevated chance of heat wave occurrence, whereas two patterns (WR2&WR3) bring cold conditions (Fig. 6b–d). These warm and cold flavors of SAWs are consistent with Gershunov et al. (2021). In the northern latitudes, WR 2–6 result in enhanced onshore flow along the northern/northwestern boundary of the ridge, bringing elevated AR probabilities for British Columbia and the Pacific Northwest (Fig. 5a).

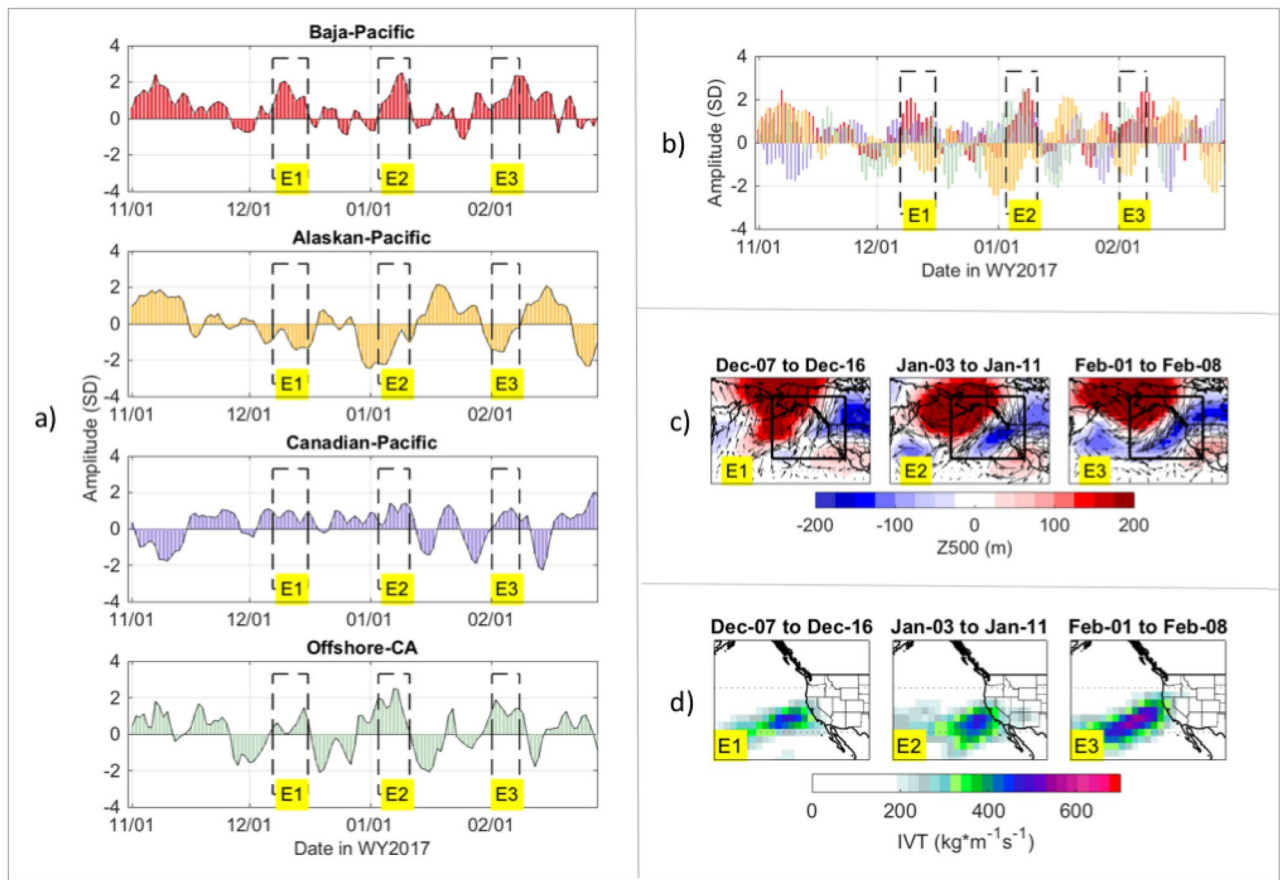


Fig. 3 Example showing the relationship between the NP4 modes and weather patterns over the North Pacific/western US during WY2017. Daily amplitudes of each mode are shown in (a). These modes can be in- or out-of-phase with each other on a given day, resulting in different phase combinations (b). Three events are identified (E1–E3) when the joint phase combination was the same: The Alaskan-Pacific mode

was negative and the other three modes were positive. Composites of Z500 and IVT for these three events are shown in (c, d), respectively. The box in (c) shows the region where the NP4 modes are most influential and where the circulation is expected to be largely modulated by the NP4 mode interaction (i.e. the composites should look similar inside the box but not necessarily outside the box)

Weather regimes 7–12 bring wetter conditions to the western US coast (Fig. 5) due to the position of an offshore trough that enhances transport of oceanic moisture over land (Fig. 2). Weather regimes 7–8 feature a trough positioned near the Pacific Northwest coastline. The location of this trough is favorable to precipitation and AR landfalls over Oregon and Washington and into Northern California. Weather regimes 9–10 feature a trough offshore California, which brings precipitation and AR landfalls over Central and Northern California. For weather regimes 11–12, the trough is further equatorward, favoring a more southerly AR track with wet conditions centered over Southern California and penetrating into the interior Southwest.

Weather regimes 15–16 bring anomalous onshore flow over Baja California (Fig. 2), with wet conditions into the Sonoran Desert region (Fig. 5). Concurrently, these weather patterns bring strong easterly/northeasterly flow to Northern California/Pacific Northwest along the eastern boundary of

a ridge poised over Alaska or British Columbia. Previous work has noted the link between ARs over Baja and inland penetration of moisture into the Desert Southwest (Rutz and Steenburgh 2012; Neiman et al. 2013; Hughes et al. 2014; Rutz et al. 2014; Rutz et al. 2021; Swales et al. 2016; Gershunov et al. 2017).

4 Atmospheric rivers, extreme precipitation, and California water resources

The weather regimes responsible for most of California's total and extreme precipitation are WR9–12 (Fig. 5c, d). WR9 is characterized by a deep and expansive trough centered over the Gulf of Alaska, with a ridge positioned over Southern California that helps to channel moisture towards Central and Northern California (Fig. 2). This weather pattern elevates AR probability threefold along the coast

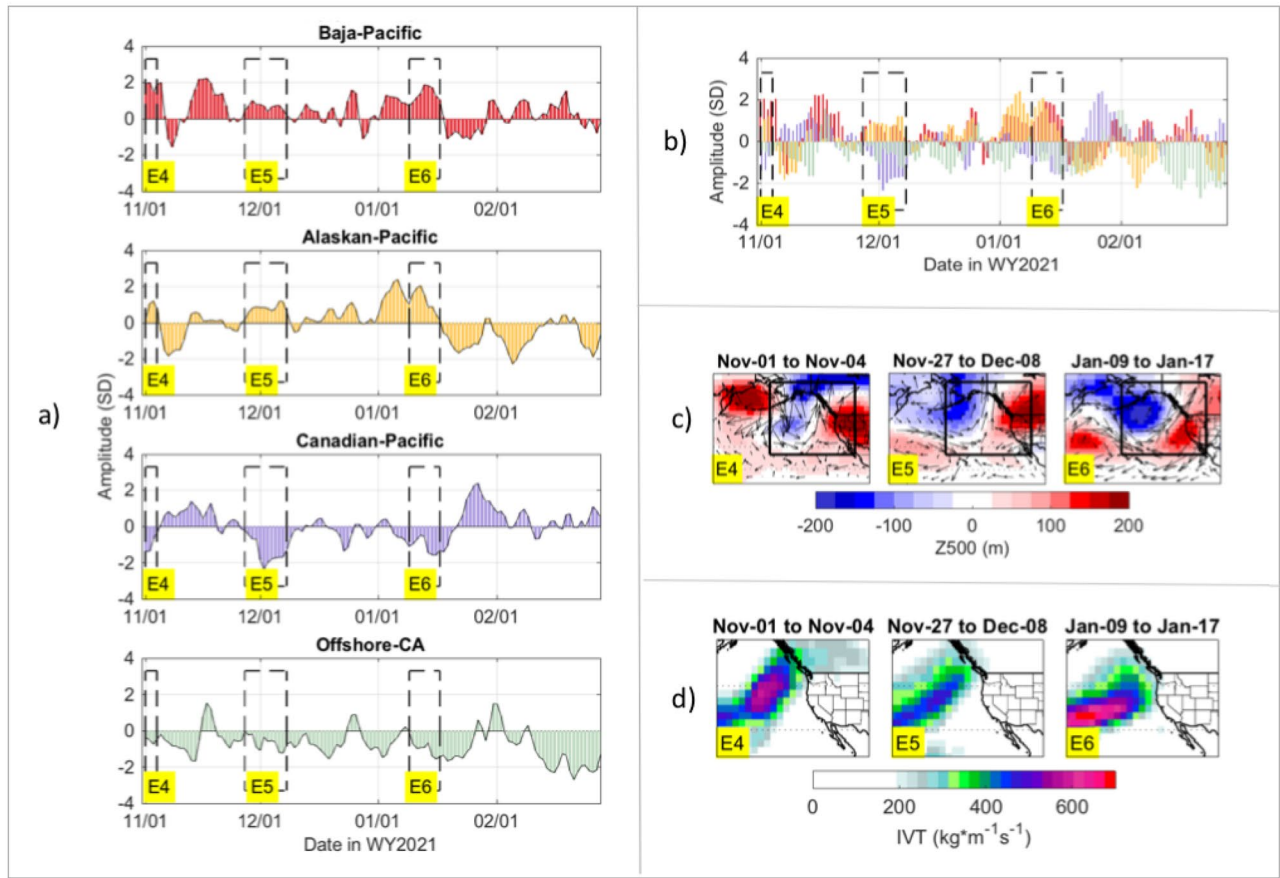


Fig. 4 As in Fig. 3 but for WY2021. Three events are identified (E4–E6) when the joint phase combination was the same: The Alaskan-Pacific and Baja-Pacific modes were positive and the Canadian-Pacific and Offshore-California modes were negative

from Central California to the Pacific Northwest (Fig. 5a) and brings a high probability of extreme precipitation (Fig. 5c). In Central and Northern California, by contributing upwards of 30% of annual precipitation, WR9 is the most important source of precipitation (Fig. 5d). WR10 is also vital for California water resources (Fig. 5d) and is an important driver of AR landfalls (Fig. 5a) and extreme precipitation (Fig. 5c). It is similar to WR9 in the position of the high and low pressure centers along the West Coast (Fig. 2). However, WR10 is characterized by a ridge over Alaska (negative phase of the Alaska-Pacific Mode) and a positively tilted trough that extends towards the tropics.

WR12 is similar to WR10, except it lacks the ridge over Southern California, which is an important distinction as its absence allows the trough to expand equatorward (Fig. 2) bringing more AR activity and precipitation to Southern California (Fig. 5). WR11 is also impactful for Southern California, bringing a high probability of extreme precipitation when it occurs (Fig. 5c), but it accounts for a smaller proportion of total SoCal precipitation (Fig. 5d) due to the lower frequency of occurrence

(i.e., WR11 is more transitory and is observed on 2% of days compared to 9% for WR12).

Figure 7 summarizes just how critical these weather patterns are to California precipitation extremes and water resources. Collectively, while they account for only 25% of November–February days, they account for up to 72% of total precipitation and up to 80% of extreme precipitation for some locations in California (Fig. 7a, b). Using the AR intensity scale of Ralph et al. (2019), we find that WR9 and WR10 are the primary synoptic weather patterns for the most intense and destructive ARs (AR scale 4 & 5, Fig. 7c). WR9 and WR10 collectively account for approximately 50% of AR category 4 storms and more than 80% of AR category 5 storms impacting California. Median flood damages associated with AR category 4 and 5 events are on the order of \$20 million and \$260 million, respectively (Corringham et al. 2019).

Previous work has shown how the presence or absence of one-to-three intense storms can make-or-break a water year (Dettinger et al. 2011) or terminate a drought (Dettinger 2013), or prevent the onset of a megadrought (Hatchett

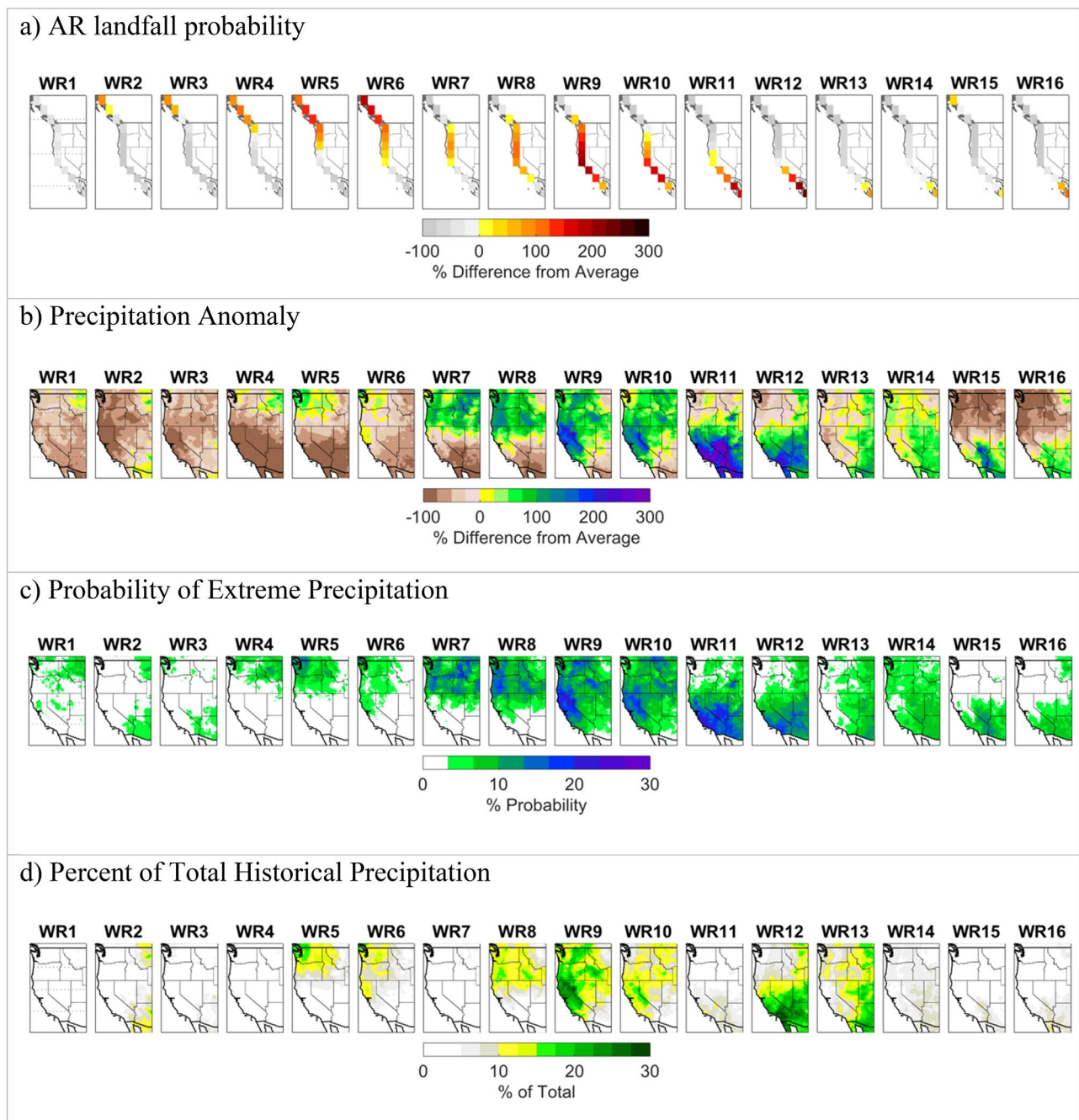


Fig. 5 Impacts associated with each weather regime showing **a** AR landfall probability, **b** precipitation anomaly, **c** probability of extreme precipitation, **d** percent of total historical precipitation. Precipitation extremes are daily accumulations above the local 95th percentile.

Sample size is important for comparing (**c, d**) where some weather regimes bring high probabilities of extreme precipitation but are less common and thus do not contribute substantially to the total historical precipitation (e.g. WR7 and WR11, see sample sizes in Fig. 2)

et al. 2016). Our findings suggest that these make-or-break storms most likely carry synoptic signatures similar to WR9–12. These few but large storms are important in building the Sierra Nevada snowpack that later melts and provides beneficial warm season water resources to meet human and ecological demands. Figure 8 shows the relationship between the seasonal frequency of WR9–12 and interannual

snowpack variability in the Northern Sierra Nevada, which demonstrates a very strong relationship between the number of days in a season that WR 9–12 were present and snow water equivalent (SWE) at Donner Summit on March 1. The relationship is strong ($p < 0.001$, $r = 0.61$) even though important details including precipitation itself or snowmelt events are not considered. This analysis used only one in-situ

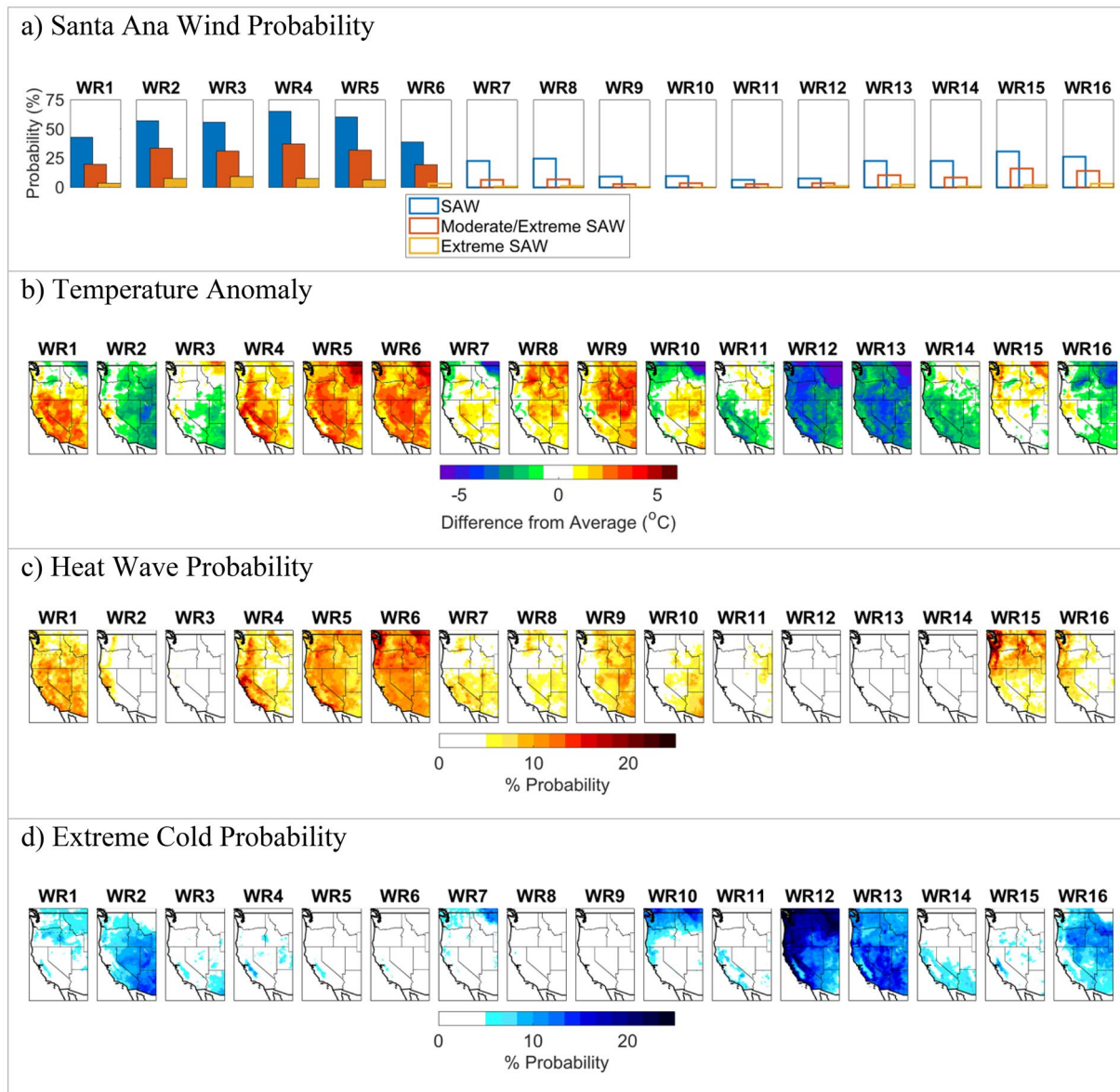


Fig. 6 Additional impacts associated with each weather regime showing **a** Santa Ana wind probabilities, **b** temperature anomalies, **c** heat wave probability, and **d** extreme cold probability. The temperature plots use daily maximum temperatures. Heat waves (cold extremes)

are defined as exceedances above (below) the historical 95th (5th) percentile after removing the seasonal cycle. Filled bars in **(a)** highlight SAW probabilities above climatology

location and a stronger relationship could emerge using a more robust SWE dataset.

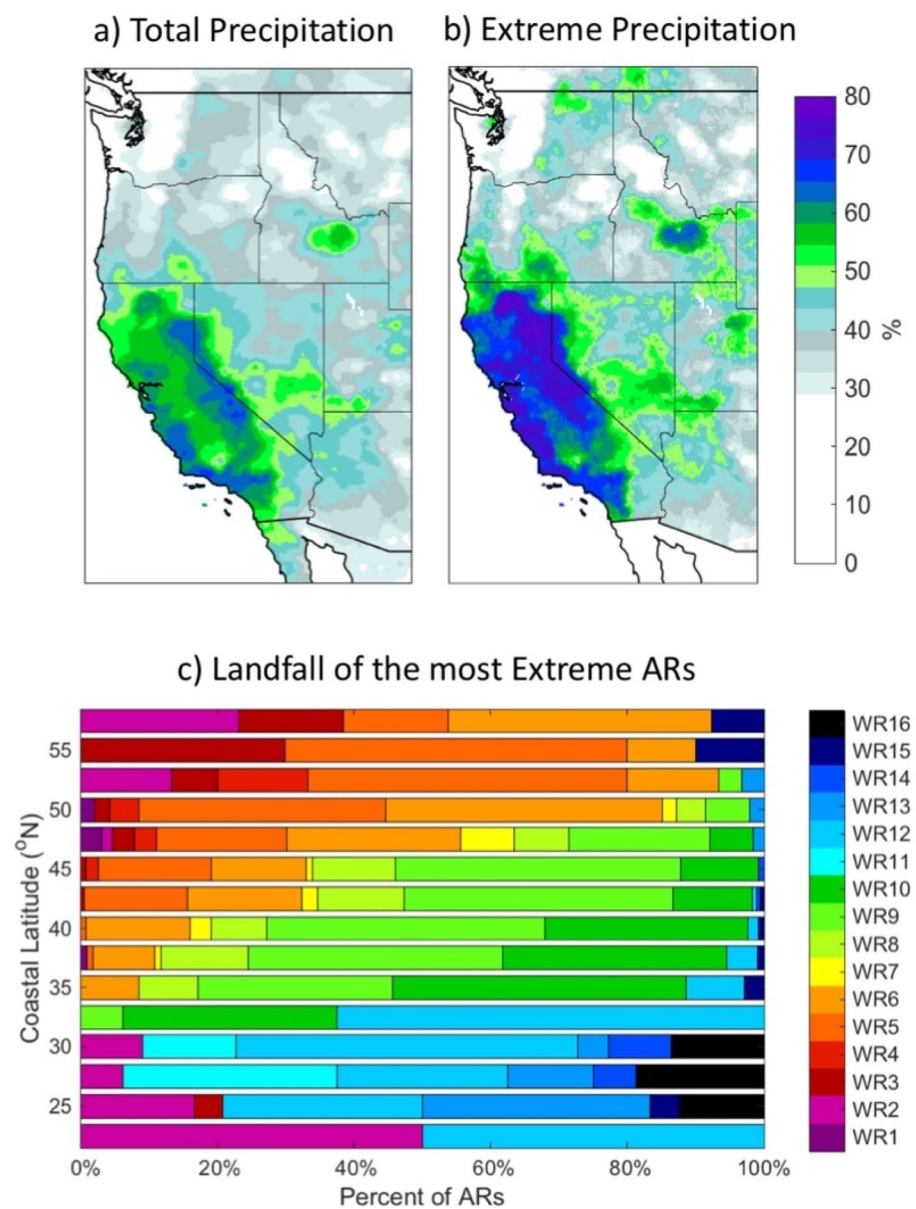
4.1 Historic California floods

We selected eight flood events to investigate from a weather regime perspective. These historic events were selected because they have achieved notoriety for the amount of destruction they caused. These are the floods of December 1955, December 1964, January 1969, February 1986,

January 1995, December/January 1996–97, February 2017, and February 2019.

Figure 9 shows the IVT magnitude during AR landfalls at different latitudes along the coast during Nov-Feb for the eight seasons when these floods occurred, classified by weather regime. For California latitudes ($32.3\text{--}42^{\circ}\text{ N}$) we see that the most intense ARs, including the historic floods (labeled F1–F8), are associated with WR9 and WR10 (See also Fig. 5). Often, the historic floods follow on the tails of one or more ARs, which prime the soil moisture, groundwater, and streamflow conditions for subsequent flooding

Fig. 7 The importance of weather regimes 9–12 for California water resources. **a** Shows the percent of total historical precipitation that occurred during WR9–12 and **b** shows the percent of historical extreme precipitation that occurred during WR9–12. **c** Gives the weather regime distribution for the most extreme ARs (scales 4 & 5) that made landfall along the west coast

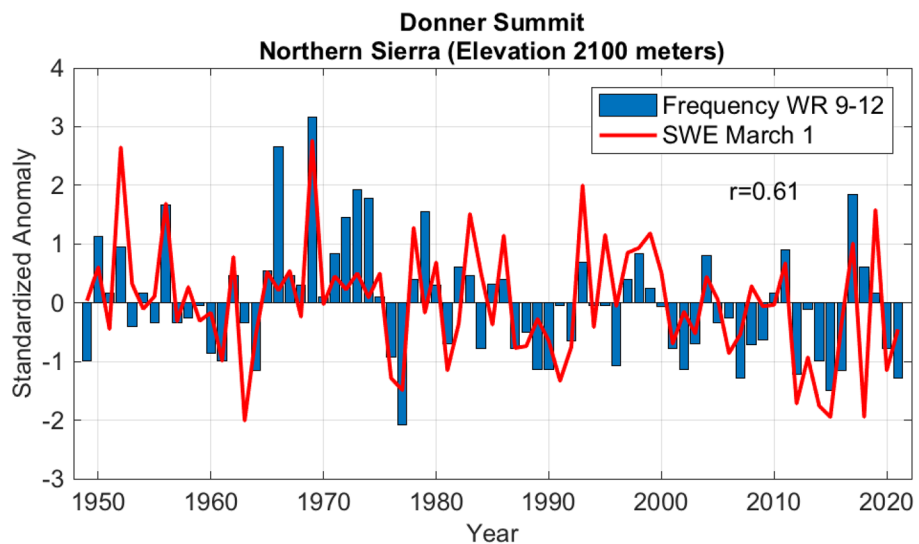


(Albano et al. 2020). Evidence of “AR Families”, as defined by Fish et al. (2019), whereby successive AR landfalls occur at the same location, are also seen (e.g. repeated ARs hitting California during 1996–97 and 2016–17 classified as WR9/10). Such “AR Families” impacting California have been linked to certain semi-stationary atmospheric circulation patterns over the North Pacific (Fish et al. 2019), which are similar in their ridge/trough positions to WR9–12.

Figure 10 shows Z500 anomalies on the peak day of each event along with the weather regime classification, where we see that all peak days are classified as either WR9 or WR10. These patterns favor very strong vapor transport over California (Fig. 11). While the patterns are similar, there are distinctions in the position of the ridge located over/near Alaska and the position/orientation of

the trough relative to the coast. The positioning of these synoptic features modulates the location of the AR track as it intersects the coast, which is critical from a local impacts perspective (e.g. note the latitudinal differences in the AR landfall location in Fig. 11). While there are slight variations in the synoptic signatures, the weather patterns represent a recurring type of atmospheric circulation linked to extreme precipitation in California, which is consistent with many studies in the literature investigating these or other extreme AR events (e.g. Weaver 1962; Estes 1994; Baker and Estes 1994; Strobin and Reynolds 1995; Ralph et al. 2004; Neiman et al. 2008; Guirguis et al. 2018, 2019, 2020a; Hatchett et al. 2020), including hypothetical cases (Porter 2011).

Fig. 8 The relationship ($r=0.61$) between snow water equivalent on March 1 at Donner Summit in the Northern Sierra and the frequency of weather regimes 9–12 during November–February



5 Santa Ana winds and fire weather

We next investigate the role of the sixteen weather patterns in driving the opposite regional weather phenomena: Santa Ana winds and wildfire. Wildfires in California are of increasing concern as recent years have brought extremely destructive and widespread wildfires with devastating loss of life and property and long periods of unhealthy air quality. The largest Southern California wildfires are typically associated with anomalously hot temperatures, dry vegetation, and persistent Santa Ana winds. Here we discuss the types of weather patterns most conducive to wildfire in California during winter.

Weather regimes 1–6 all support offshore flow over Southern California (Fig. 2) and SAW probabilities in the range of 39–65%, or 20–100% above average (Fig. 6a). These six patterns are also anomalously dry for California generally (Fig. 5), although WR6 can produce AR impacts in Northern California (Fig. 5a) in cases when the offshore trough (Fig. 2) moves closer to shore.

Two of these patterns are associated with cold SAWs (WR2&3), and the rest are hot SAW patterns with elevated chances of a heat wave (Fig. 6). Hot SAWs are associated with a ridge centered over the Great Basin, while cold SAWs feature a trough over the interior Southwest and a positively tilted offshore ridge that brings northeasterly flow to coastal California (Figure S3). The synoptic signatures associated with hot and cold flavors of SAWs are consistent with recent findings (Gershunov et al. 2021).

Figure 12 shows the weather regime distribution for start dates of the largest Southern California wildfires. As expected, the weather regimes associated with SAWs (WR1-6) are those responsible for most (78%) large wildfire starts, and the hot SAW patterns are responsible for more than twice as many starts (58%) as cold SAWs

(24%). Gershunov et al. (2021) found hot SAWs to be responsible for the largest wildfire acreages burned in Southern California, partly because hot SAWs tend to last longer and their high temperatures support enhanced drying of vegetation and lower relative humidity, but also because cold SAWs tend to be preceded by precipitation. Weather regime 5 is associated with the largest number of wildfire ignitions (30%), which results from strong offshore flow (Fig. 2) favoring fire weather: hot, dry, SAW conditions (Figs. 5, 6). The WR5 pattern also occurs more frequently than other hot, dry, SAW patterns (i.e. WR5 occurs on 10% of days compared to 3% for each WR1 and WR4). Composites of atmospheric circulation associated with Southern California wildfire start days classified as WR1-6 (Figure S4) highlight the similarity between synoptic circulation on specific wildfire start days and the defined weather regimes (Fig. 2).

5.1 The California Thomas Fire of 2017

In addition to hot, dry, and windy conditions needed for a wildfire to grow, the largest wildfires are associated with the persistence of these conditions over a period of time without rain. The Thomas Fire of 2017–2018 burned for over a month, igniting December 4 before being fully contained on January 12. Figure 13a shows atmospheric river activity during 2017–2018, highlighting ARs hitting land between 22.5 and 57.7° N. We see that AR landfalls occurred along the West Coast in November of 2017 (seen as green circles mostly north of 35°), but these storms primarily impacted the Pacific Northwest and Northern California, while Southern and Central California remained dry. December is typically the most active month for ARs in Northern California and the second most active month for ARs in Southern California (Gershunov et al. 2017). However, in December

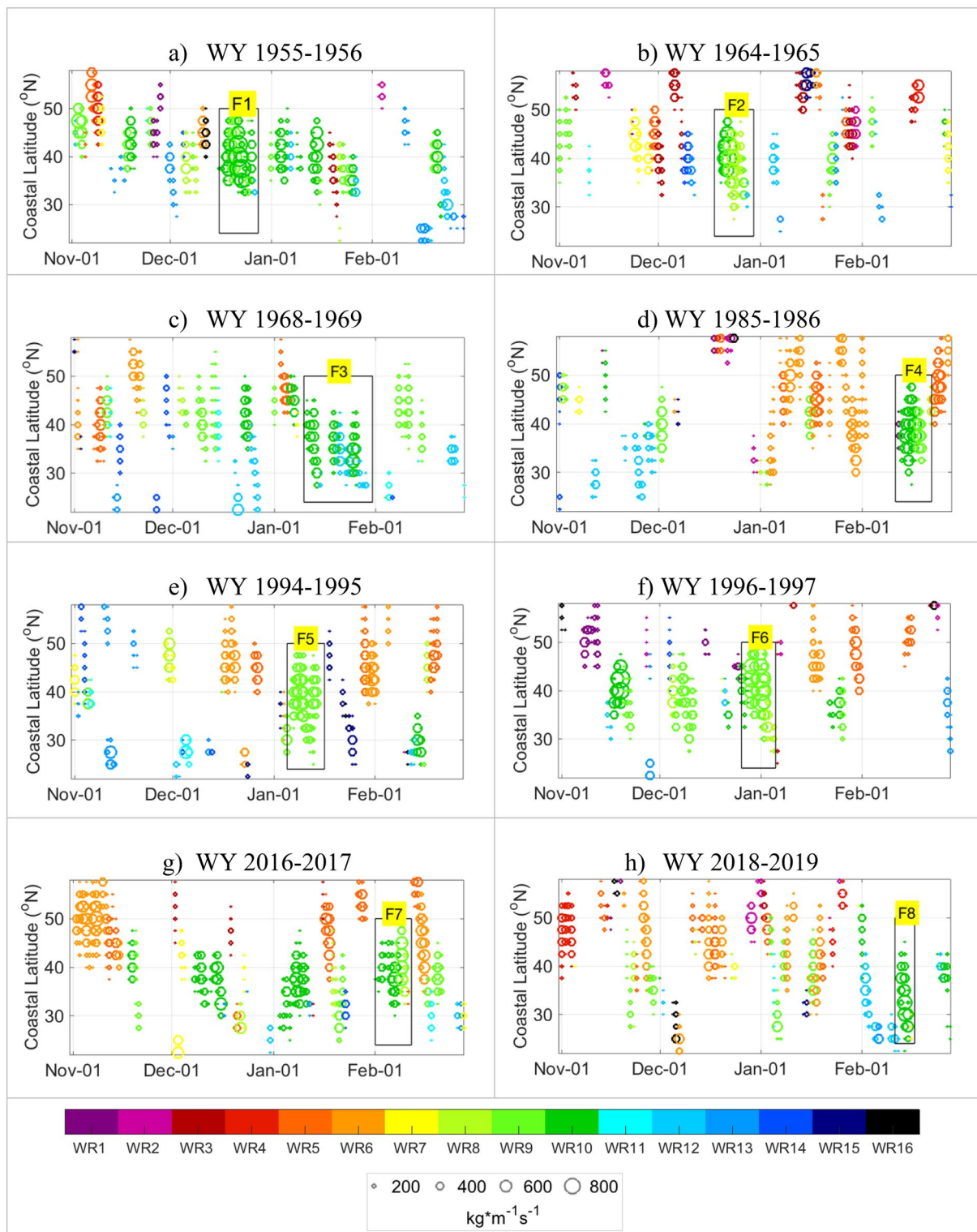


Fig. 9 AR landfalls during select water years when historical floods occurred, where the y-axis gives the coastal latitude and the x-axis gives the date in the season. The marker size shows the magnitude of AR IVT (daily average) and the color scale gives the weather regime

observed for each day. Eight flood events (F1-F8) are highlighted for further discussion. Daily IVT magnitudes less than $250 \text{ kg} \cdot \text{m}^{-1} \cdot \text{s}^{-1}$ signify days when an AR was observed for only part of the day

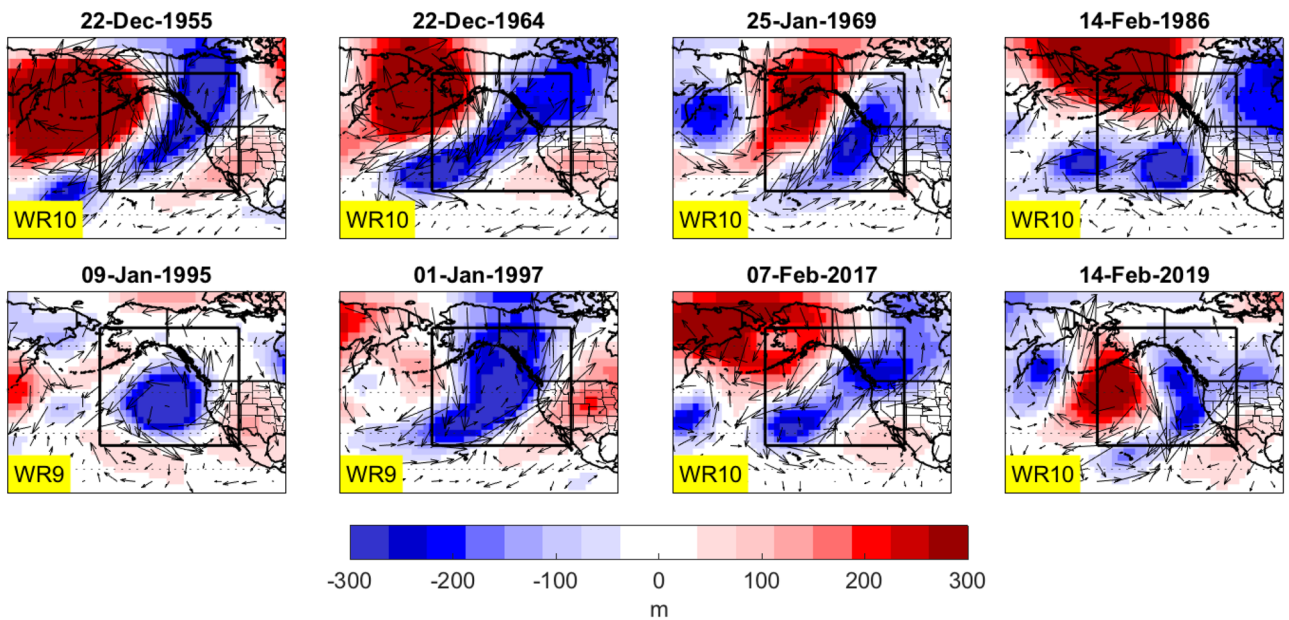


Fig. 10 Observed Z500 anomalies for the day with the most intense AR footprint over California for each flood event, defined by the summed IVT over California. The weather regime classification for each day is given as highlighted text in the lower left corner of each map

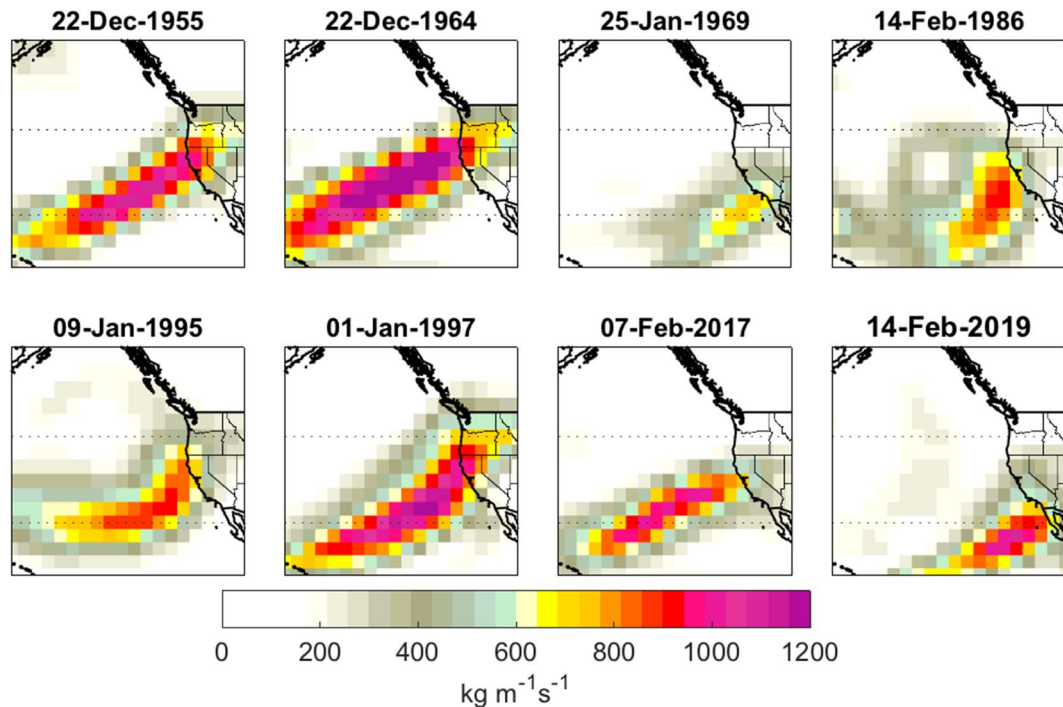


Fig. 11 Observed IVT for the same days shown in Fig. 10

2017 no ARs made landfall in the State. Following ignitions by downed power lines on and around December 4, the dominant weather patterns were those associated with hot, dry, SAW conditions. From Fig. 13b, the most common weather regimes during December 4–January 12 were WR1

(11 days), WR4 (6 days), WR5 (6 days), and WR6 (5 days). Containment of the fire was aided by a weak atmospheric river on January 9–10 (classified as WR8, Fig. 13a). While this storm finally brought rainfall, it also brought tragedy as it included short-duration, high intensity precipitation

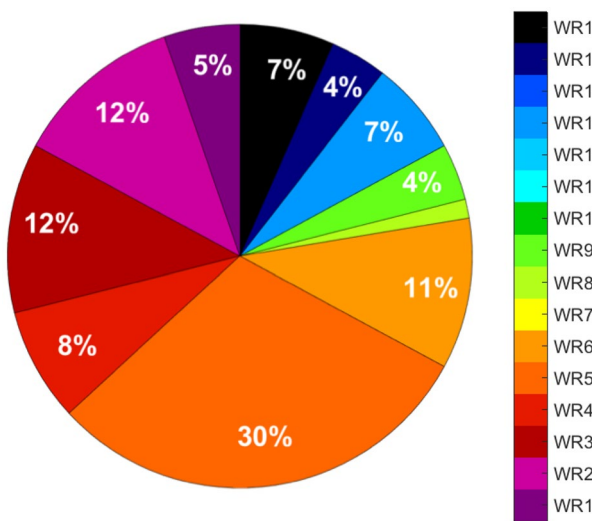


Fig. 12 The weather regime distribution of Southern California wildfire starts

associated with cold frontal passage that triggered fatal post-fire debris flows in the coastal community of Montecito (Oakley et al. 2018).

6 Observed trends in weather regime frequency and implications for California water resources and fire hazard

In the past decade, California has endured two extreme and persistent droughts, ongoing extreme heat, and eight of the ten largest wildfires in over a century of records (Krishnamoorthy and Kannan 2020). Here, we investigate if and how winter weather patterns are changing across the western US, and how these changes might affect winter weather variability and extremes in California. Figure 14 gives the seasonal frequency of each weather regime over the historical record, along with statistically significant ($p < 0.05$) increasing (red) and decreasing (blue) trends. The weather patterns found to be increasing in frequency are WR1, WR4, WR5, and WR7. While WR7 is not linked to extreme California weather in our analysis, the other three weather regimes (1, 4 & 5) are major contributors to historical wildfires (Figs. 12 and 13b) and are associated with heat waves in California and the western US (Fig. 6c). The combined seasonal frequency of these three weather regimes is provided in Fig. 15b, which shows a strong increase in the frequency of these impactful weather patterns (slope = 0.21% per year, $p < 0.001$). During the 2021 water year, which was the second driest statewide in 125 years (California Department of Water Resources 2021), these weather patterns accounted for 41% of days in the season. This anomaly was exceeded only once previously in 2015, also a critically dry year in California and Nevada (Sterle et al. 2019; Western Regional Climate Center 2021).

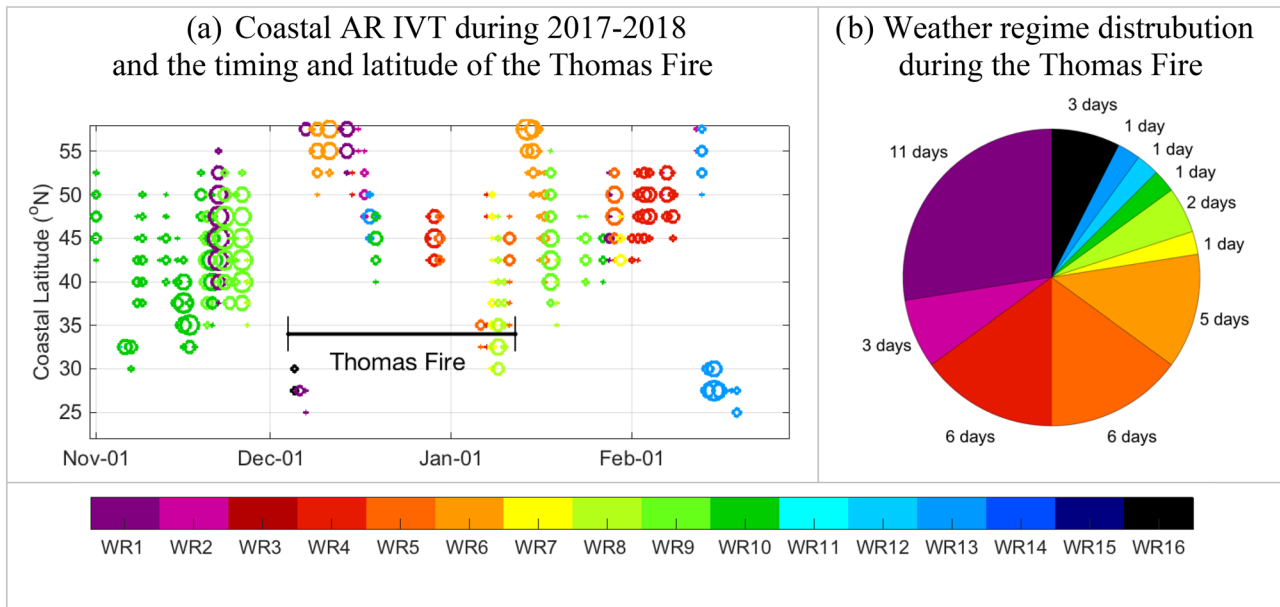


Fig. 13 As in Fig. 9 but for the 2017–2018 season and showing the timing and latitude of the Thomas Fire (a). The weather regime distribution from the ignition date to full containment (December 4–January 12) is shown in (b)

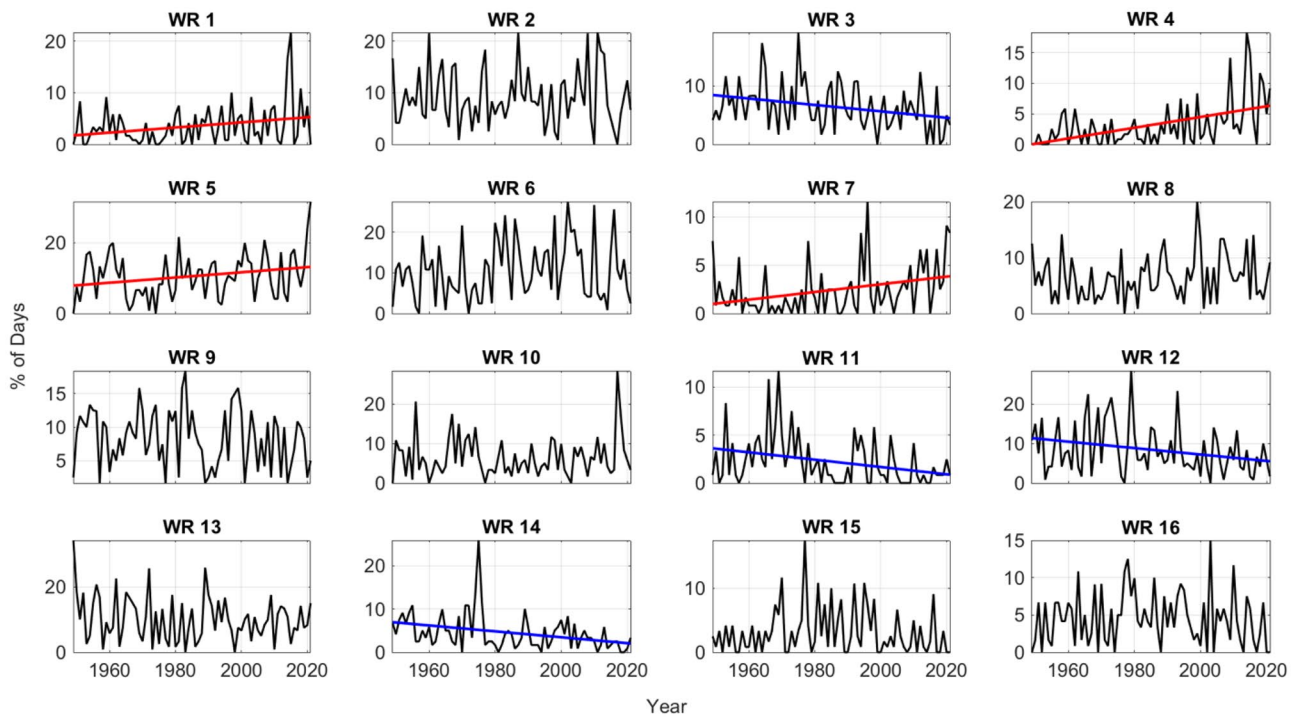


Fig. 14 Observed frequency of each weather regime during Nov–Feb (black) and statistically significant ($p < 0.05$) trends colored red for increasing trends or blue for decreasing trends

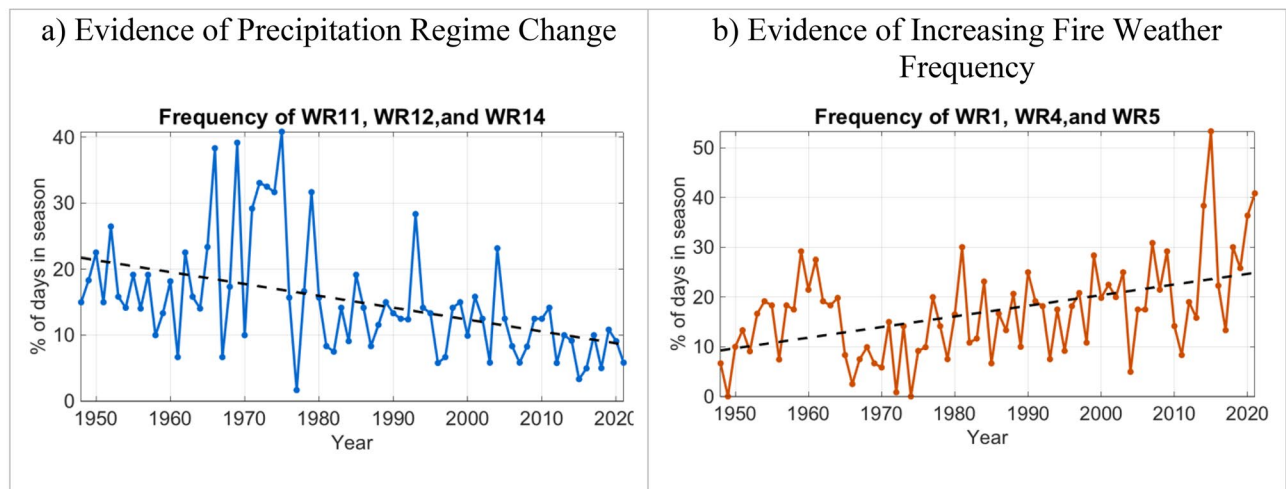


Fig. 15 The combined seasonal frequency of WR11, WR12, and WR14 with the long-term trend (a), and the combined seasonal frequency and trend of WR1, WR4, and WR5 (b). Both trends are statistically significant ($p < 0.001$)

Along with increasing fire hazard due to the rising frequency of hot, dry, SAW patterns, we also find evidence of decreasing frequency of weather patterns associated with cold SAWs (WR3; see also Gershunov et al. 2021) and precipitation in the Southwest (WR11, WR12, and WR14). Figure 15a shows the combined frequency of the patterns associated with southwest precipitation (WR11, WR12, and

WR14, slope = -0.18% per year, $p < 0.001$). These are all associated with a deep trough over and offshore from western North America (Fig. 2) with moisture transport along a southern track bringing precipitation to Southern California and the Desert Southwest (Fig. 5). These weather regimes also tend to be colder (Fig. 6b, d), therefore this decreasing trend could mean less precipitation in general, but also less

cold precipitation which has implications for snow accumulation and storage. We find no long-term trends for the weather patterns associated with the strongest ARs and the most destructive California floods (WR9 and WR10). This suggests that atmospheric circulation is changing to favor fire weather at the expense of precipitation in Southern California, but the hazard of extreme precipitation and flooding caused by the strongest ARs is not diminishing.

The observed trends in the frequency of certain weather patterns is related to the rising frequency of ridging over land along the west coast. Specifically, we observe a positive trend in the Baja-Pacific mode, which makes ridging over Baja California more likely, and a negative trend in the Canadian-Pacific mode, which corresponds to an increase in ridging over the Pacific Northwest and western Canada (Figs. S5 and 1a). These geospatial differences in trends of height anomalies over land relative to those over the Pacific Ocean favor atmospheric blocking conditions associated with dry weather in California. Persistent ridging has been implicated in recent California droughts (e.g., Swain et al. 2014; Bond et al. 2015; Gibson et al. 2020a).

7 Discussion

In this study, we demonstrate how four modes of atmospheric circulation over the North Pacific Ocean interact to produce distinct weather patterns that recur throughout the historical record. These recurring weather patterns drive AR landfalls, extreme precipitation, historic floods, Santa Ana winds, wildfires, and temperature extremes during California winters. Relationships between the driving NP4 modes and climate-scale teleconnections like ENSO have already been discovered (GGR'20) and the results presented here provide a method for exploring important linkages between seasonal- and weather-scale processes that could help to improve predictability of extreme events. This methodology can easily be applied to dynamical weather forecast models to investigate the predictability of extreme weather impacts at S2S lead times. Predicting the phase of one or more NP4 modes, using dynamical, statistical, or hybrid methods, would be highly useful for situational awareness regarding the likelihood of extreme weather events. Dynamical models have been shown capable of producing skillful forecasts of large-scale circulation features at lead times of 2.5 weeks (e.g. Ferranti et al. 2018, 2019) to several weeks (Gibson et al. 2020b). Additional lead time and higher confidence in long-lead forecasts can be translated by forecasters into improved impact-based decision support (Uccellini and Hoeve 2019) to partner agencies and used to provide earlier warning to the public before extreme events (e.g., Lambrecht et al. 2019, 2021).

An important outcome of this work is the generation of a catalog of daily weather patterns spanning 73-years (Guirguis et al. 2022), which can be used for monitoring and predictability studies. Our weather regime classification has been shown to be skillful at representing important circulation features associated with impactful events, including destructive floods and Southern California wildfires. Using this approach, we find that the seasonal frequency of weather patterns associated with wildfire is increasing while other patterns that bring precipitation to southern California and the Desert Southwest are decreasing in frequency. This is an unsettling set of trends, as during 2020 California suffered its worst wildfire season on record, causing extensive impacts to ecosystems, property, and public health (e.g. Aguilera et al. 2020, 2021). The continued dry conditions experienced during winter 2020–2021 exacerbated already extreme fire hazards throughout California. Significant wildfire activity occurred in the Sierra Nevada and northern Coastal Ranges during the summer and fall of 2021, however two early-winter precipitation events largely reduced Southern California fire hazard and luckily no major fires occurred during the SAWs that did occur.

Importantly, while circulation changes appear to be reducing the likelihood of some types of precipitation events (WR11, WR12, WR14), there is no observed change in the weather patterns responsible for the most intense ARs and destructive floods (WR9 and WR10). With warming due to anthropogenic climate change, these patterns could potentially be even more destructive as the atmosphere can more effectively transport larger quantities of water vapor (Rhoades et al. 2021). This is consistent with recent work focused on precipitation regime changes in California using climate model projections (Pierce et al. 2013; Polade et al. 2017; Espinoza et al. 2018; Swain et al. 2018; Gershunov et al. 2019), which suggest that future California precipitation will come by way of fewer, more intense storms with longer dry spells in between. While the trends detected in this study are sensitive to the record length of the observations, the methodology could be applied to climate model projections to evaluate the roles of natural variability versus climate change in driving the recent changes in weather regime frequency.

There are many research questions that could be explored using this methodology and data catalog. While we provided only a cursory look at the relationships with snowpack, the role of different weather patterns in driving snow accumulation and depletion throughout the western United States, would be valuable knowledge from a water resource perspective, particularly as snowpack continues to decline (Siirila-Woodburn et al. 2021). In this work, we explicitly focused on Southern California's SAWs while recognizing the importance of Diablo winds in Northern California. Recent work suggests that Northern

California's Diablo winds are dynamically related and tend to co-occur with SAWs (Gershunov et al. 2021). This weather regime approach and catalog would be useful for exploring the coordination of California's downslope wind systems in detail.

Further investigation on the timing and transition of different weather patterns could provide insight for S2S predictability. While this analysis focused on the California winter season, the methodology could be applied to other seasons to study warm season heat waves and/or fire weather, as well as to other regions. Improving our understanding of the linkages between climate change, seasonal-scale teleconnections, and extreme weather will be critical for effective emergency planning, resource management, and climate change adaptation efforts at local, regional, and state levels.

Supplementary Information The online version contains supplementary material available at <https://doi.org/10.1007/s00382-022-06361-7>.

Funding This research was funded by the U.S. Department of the Interior via the Bureau of Reclamation ([USBR-R15AC00003](#)), the California Department of Water Resources ([4600010378 UCOP2-11](#)), and by the Regional Integrated Sciences and Assessments (RISA) California–Nevada Climate Applications Program and the International Research Applications Program of the National Oceanic and Atmospheric Administration (awards [NA17OAR4310284](#) and [A18OAR4310341](#)). Additional funding was provided by the University of California Office of the President MRP1 grant MRP-17-446315. This study contributes to DOI's Southwest Climate Adaptation Science Center activities and NOAA's California and Nevada Applications Program award [NA11OAR43101](#).

Availability of data and material The winter weather regimes catalog developed for this study is available from the UC San Diego Library Digital Collections at <https://doi.org/10.6075/J089161B> (Guirguis et al. 2022). The NP4 dataset is available at <https://doi.org/10.6075/J0154FJJ> (Guirguis et al. 2020b). The Santa Ana winds regional index and the SIO-R1 AR catalog are available at <https://weclima.ucsd.edu/data-products/>. The Livneh temperature and precipitation data are available at <https://climatedataguide.ucar.edu/climate-data>. Wildfire information is from the California Fire Protection's Fire and Resource Assessment Program (FRAP) fire perimeters database available at <https://frap.fire.ca.gov/frap-projects/fire-perimeters/>. Snow water equivalent for the Sierra Nevada are from the Natural Resources Conservation Service available at <https://wcc.sc.egov.usda.gov/nwcc/rgrpt?report=snowcourse&state=CA>. Code availability Code developed for this study will be made available upon request.

Declarations

Conflict of interest The authors declare no competing interests.

Open Access This article is licensed under a Creative Commons Attribution 4.0 International License, which permits use, sharing, adaptation, distribution and reproduction in any medium or format, as long as you give appropriate credit to the original author(s) and the source, provide a link to the Creative Commons licence, and indicate if changes were made. The images or other third party material in this article are included in the article's Creative Commons licence, unless indicated otherwise in a credit line to the material. If material is not included in the article's Creative Commons licence and your intended use is not permitted by statutory regulation or exceeds the permitted use, you will need to obtain permission directly from the copyright holder. To view a copy of this licence, visit <http://creativecommons.org/licenses/by/4.0/>.

References

- Abatzoglou JT, Barbero R, Nauslar NJ (2013) Diagnosing Santa Ana winds in Southern California with synoptic-scale analysis. *Wea Forecast* 28:704–710. <https://doi.org/10.1175/WAF-D-13-00002.1>
- Abatzoglou JT, McEvoy DJ, Redmond KT (2017) The west wide drought monitoring at fine spatial scales. *BAMS* 98(9):1815–1820
- Abatzoglou JT, Hatchett BJ, Fox-Hughes P, Gershunov A, Nauslar NJ (2021) Global climatology of synoptically-forced downslope winds. *Int J Climatol* 41(1):31–50
- Aguilera R, Hansen K, Gershunov A, Ilango S, Sheridan P, Benmarhnia T (2020) Respiratory Hospitalizations and Wildfire Smoke: a spatio-temporal analysis of an extreme firestorm in San Diego County, California. *Environ Epidemiol*. <https://doi.org/10.1097/EDE.0000000000000114>
- Aguilera R, Corringham T, Gershunov A, Benmarhnia T (2021) Wildfire smoke impacts respiratory health much more than fine particles from other sources: observational evidence from Southern California. *Nat Commun* 12:1493. <https://doi.org/10.1038/s41467-021-21708>
- Albano CM, Dettinger MD, Harpold AA (2020) Patterns and Drivers of Atmospheric River Precipitation and Hydrologic Impacts across the Western United States. *J Hydrometeorol* 21(1):143–159
- Amini S, Straus DM (2019) Control of storminess over the pacific and North America by circulation regimes. *Clim Dyn* 52:4749–4770. <https://doi.org/10.1007/s00382-018-4409-7>
- Baker D, Estes G (1994) Using the TEREC Pattern to Predict Heavy Rainfall in California. Proceedings of 1994 California Weather Symposium. <https://cepsym.org/Sympro1994/Baker.pdf>. Accessed 1 Sept 2021
- Barnston AG, Livezey RE (1987) Classifications, seasonality, and persistence of low-frequency atmospheric circulation patterns. *Mon Weather Rev* 115:1083–1126. [https://doi.org/10.1175/1520-0493\(1987\)115%3c1083:CSAPOL%3e2.0.CO;2](https://doi.org/10.1175/1520-0493(1987)115%3c1083:CSAPOL%3e2.0.CO;2)
- Bond NA, Corin MF, Freeland H, Mantua N (2015) Causes and impacts of the 2014 warm anomaly in the NE Pacific. *Geophys Res Lett* 42:3414–3420. <https://doi.org/10.1002/2015GL063306>
- California Department of Water Resources (2021) Water Year 2021: An Extreme Year. [Available online at https://water.ca.gov/-/media/DWR-Website/Web-Pages/Water-Basics/Drought/Files/Publications-And-Reports/091521-Water-Year-2021-broch_v2.pdf]
- Chediak M, Sullivan BK (2021) Californians Suffer Unprecedented Fire Blackouts in January. Bloomberg Green, 16 January, 2021, <https://www.bloomberg.com/news/articles/2021-01-17/parched-california-braces-for-winter-fire-season-blackouts>. Accessed 19 July 2021
- Corringham TW, Ralph FM, Gershunov A, Cayan DR, Talbot CA (2019) Atmospheric Rivers drive flood damages in the western United States. *Sci Adv* 5(12):eaaz631. <https://doi.org/10.1126/sciadv.aax4631>

- Dettinger MD (2013) Atmospheric Rivers as Drought Busters on the U.S. West Coast. *J Hydrometeorol* 14(6):1721–1732
- Dettinger MD, Ralph FM, Das T, Neiman PJ, Cayan DR (2011) Atmospheric rivers, floods and the water resources of California. *Water* 3(2):445–478
- Espinosa V, Waliser DE, Guan B, Lavers DA, Ralph FM (2018) Global analysis of climate change projection effects on atmospheric rivers. *Geophys Res Lett.* <https://doi.org/10.1029/2017GL076968>
- Estes G (1994) Weather patterns and American River Floods. <https://cepsym.org/Sympro1998/Estes.pdf>. Accessed 1 Sept 2021
- Ferranti L, Magnusson L, Vitart F, Richardson DS (2018) How far in advance can we predict changes in large-scale flow leading to severe cold conditions over Europe? *QJRMS* 144:1788–1802. <https://doi.org/10.1002/qj.3341>
- Ferranti L, Magnusson L, Vitart F, Richardson DA (2019) A new product to flag up the risk of cold spells in Europe weeks ahead. *ECMWF Newsletter No. 158*, pp 15–20
- Fish MA, Wilson AM, Ralph FM (2019) Atmospheric river families: definition and associated synoptic conditions. *J Hydrometeorol* 20:2091–2108. <https://doi.org/10.1175/JHM-D-18-0217.1>
- Gershunov A, Guirguis K (2012) California heat waves in the present and future. *Geophys Res Lett* 39:L18710. <https://doi.org/10.1029/2012GL052979>
- Gershunov A, Shulgina T, Ralph FM, Lavers D, Rutz JJ (2017) Assessing the climate-scale variability of Atmospheric Rivers affecting the west coast of North America. *Geophys Res Lett.* <https://doi.org/10.1002/2017GRL074175>
- Gershunov A, Shulgina TM, Clemesha RES, Guirguis K, Pierce DW, Dettinger MD, Lavers DA, Cayan DR, Polade SD, Kalansky J, Ralph FM (2019) 2019: Precipitation regime change in Western North America: The role of Atmospheric Rivers. *Sci Rep* 9:9944. <https://doi.org/10.1038/s41598-019-46169-w>
- Gershunov A, Guzman Morales J, Hatchett B, Aguilera R, Shulgina T, Guirguis K, Abatzoglou J, Cayan D, Pierce D, Williams P, Small I, Clemesha R, Schwarz L, Benmarhnia T, Tardy A (2021) Hot and cold flavors of southern California's Santa Ana winds: their causes, trends, and links with wildfire. *Clim Dyn.* <https://doi.org/10.1007/s00382-021-05802-z>
- Gibson PB, Waliser DE, Guan B, DeFlorio MJ, Ralph FM, Swain DL (2020a) Ridging associated with drought in the Western and Southwestern United States: characteristics, trends, and predictability sources. *J Clim.* <https://doi.org/10.1175/JCLI-D-19-0439.1>
- Gibson PB, Waliser DE, Goodman A, DeFlorio MJ, Delle Monache L, Molod A (2020b) Subseasonal-to-seasonal hindcast skill assessment of ridging events related to drought over the Western United States. *J Geophys Res Atmos* 125:55. <https://doi.org/10.1029/2020JD033655>
- Guirguis K, Gershunov A, Clemesha RES, Shulgina T, Subramanian AC, Ralph FM (2018) Circulation drivers of atmospheric rivers at the North American West Coast. *Geophys Res Lett* 45:12–576. <https://doi.org/10.1029/2018GL079249>
- Guirguis K, Gershunov A, Shulgina TM, Clemesha RES, Ralph FM (2019) Atmospheric Rivers impacting Northern California and their modulation by a variable climate. *Clim Dyn.* <https://doi.org/10.1007/s00382-018-4532-5>
- Guirguis K, Gershunov A, DeFlorio MJ, Shulgina T, Delle Monache L, Subramanian AC, Corringham TW, Ralph FM (2020a) Four atmospheric circulation regimes over the North Pacific and their relationship to California precipitation on daily to seasonal timescales. *GRL.* <https://doi.org/10.1029/2020GL087609>
- Guirguis K, Gershunov A, DeFlorio MJ, Shulgina T, Delle Monache L, Subramanian AC et al (2020b) Data from: Four atmospheric circulation regimes over the North Pacific and their relationship to California precipitation on daily to seasonal timescales. UC San Diego Library Digital Collections. <https://doi.org/10.6075/J0154FJJ>
- Guirguis K, Gershunov A, Hatchett B, Shulgina T, DeFlorio MJ, Subramanian AC, Guzman-Morales J, Aguilera R, Clemesha R, Corringham TW, Delle Monache L, Reynolds D, Tardy A, Small I, Ralph FM (2022) Historical catalog of winter weather regimes impacting California, 1949–2017. UC San Diego Library Digital Collections. <https://doi.org/10.6075/J089161B>
- Guzman Morales J, Gershunov A (2019) Climate change suppresses Santa Ana Winds of Southern California and sharpens their seasonality. *GRL.* <https://doi.org/10.1029/2018GL080261>
- Guzman Morales J, Gershunov A, Theiss J, Li H, Cayan DR (2016) Santa Ana Winds of southern California: their climatology, extremes, and behavior spanning six and a half decades. *Geophys Res Lett.* <https://doi.org/10.1002/2016GL067887>
- Hatchett BJ, Boyle DP, Garner CB, Kaplan ML, Putnam AE, Bassett S (2016) Magnitude and frequency of wet years under a megadrought climate in the western Great Basin, USA. *Quatern Sci Rev* 152:197–202. <https://doi.org/10.1016/j.quascirev.2016.09.017>
- Hatchett BJ, Cao Q, Dawson PB, Ellis CJ, Hecht CW, Kawzenuk B et al (2020) Observations of an extreme atmospheric river storm with a diverse sensor network. *Earth Sp Sci* 7:e2020EA001129. <https://doi.org/10.1029/2020EA001129>
- Hecht CW, Cordeira JM (2017) Characterizing the influence of atmospheric river orientation and intensity on precipitation distributions over North Coastal California. *Geophys Res Lett* 44:9048–9058. <https://doi.org/10.1002/2017GL074179>
- Henn B, Musselman KN, Lestak L, Ralph FM, Molotch NP (2020) Extreme runoff generation from atmospheric river driven snowmelt during the 2017 Oroville Dam spillways incident. *Geophys Res Lett* 47(14):e2020GL088189
- Hu H, Dominguez F, Wang Z, Lavers DA, Zhang G, Ralph F (2017) Linking atmospheric river hydrological impacts on the U.S. West coast to Rossby wave breaking. *J Clim* 30:3381–3399. <https://doi.org/10.1175/JCLI-D-16-0386.1>
- Hughes M, Hall A (2010) Local and synoptic mechanisms causing Southern California's Santa Ana winds. *Clim Dyn* 34(6):847–857
- Hughes M, Mahoney KM, Neiman PJ, Moore BJ, Alexander M, Ralph FM (2014) The landfall and inland penetration of a flood-producing atmospheric river in Arizona. Part II: sensitivity of modeled precipitation to terrain height and atmospheric river orientation. *J Hydrometeorol* 15(5):1954–1974
- Kalnay E, Kanamitsu M, Kistler R, Collins W, Deaven D, Gandin L, Iredell M, Saha S, White G, Woollen J, Zhu Y, Chelliah M, Ebisuzaki W, Higgins W, Janowiak J, Mo KC, Ropelewski C, Wang J, Leetmaa A, Reynolds R, Jenne R, Joseph D (1996) The NCEP/NCAR 40-year reanalysis project. *Bull Am Meteorol Soc* 77(3):437–472
- Kanamaru H, Kanamitsu M (2007) Fifty-seven-year California reanalysis downscaling at 10 km (CaRD10). Part II: comparison with North American Regional Reanalysis. *J Clim* 20(22):5572–5592
- Kolden C, Abatzoglou J (2018) Spatial distribution of wildfires ignited under katabatic versus non-katabatic winds in Mediterranean Southern California USA. *Fire* 1(2):19. <https://doi.org/10.3390/fire1020019>
- Krishnakumar P, Kannan S (2020) The worst fire season ever. Again. *New York Times*, 15 September 2020. <https://www.latimes.com/projects/california-fires-damage-climate-change-analysis>. Accessed 19 July 2021
- Lambrecht KM, Hatchett BJ, Walsh LC, Collins M, Tolby Z (2019) Improving visual communication of weather forecasts with rhetoric. *Bull Am Meteorol Soc* 100(4):557–563
- Lambrecht K, Hatchett BJ, VanderMolen K, Feldkircher B (2021) Identifying community values related to heat: recommendations for forecast and health risk communication. *Geosci Commun* 4:517–525. <https://doi.org/10.5194/gc-4-517-2021>
- Livneh B, Rosenberg EA, Lin C, Nijssen B, Mishra V, Andreadis KM, Maurer EP, Lettenmaier DP (2013) A long-term hydrologically

- based dataset of land surface fluxes and states for the conterminous United States: update and extensions. *J Clim* 26:9384–9392
- Livneh B, Bohn T, Pierce D et al (2015) A spatially comprehensive, hydrometeorological data set for Mexico, the U.S., and Southern Canada 1950–2013. *Sci Data* 2:150042. <https://doi.org/10.1038/sdata.2015.42>
- Moritz M, Moody TJ, Krawchuk M, Hughes M, Hall A (2010) Spatial variation in extreme winds predicts large wildfire locations in chaparral ecosystems. *Geophys Res Lett* 37:L04801. <https://doi.org/10.1029/2009GL041735.1>
- Mundhenk BD, Barnes EA, Maloney ED, Nardi KM (2016) Modulation of atmospheric rivers near Alaska and the US West Coast by northeast Pacific height anomalies. *J Geophys Res-Atmos* 121:12751–12765
- Murphy P (2021) Preventing wildfires with power outages: the growing impacts of California's Public Safety Power Shutoffs. Physicians, Scientists, and Engineers for Healthy Energy Blog. <https://www.psehealthyenergy.org/news/blog-posts/>
- Neiman PJ, Ralph FM, Wick GA, Lundquist JD, Dettinger MD (2008) Meteorological characteristics and overland precipitation impacts of atmospheric rivers affecting the West Coast of North America based on eight years of SSM/I satellite observations. *J Hydrometeorol* 9:22–47
- Neiman PJ, Ralph FM, Moore BJ, Hughes M, Mahoney KM, Cordeira JM, Dettinger MD (2013) The landfall and inland penetration of a flood-producing atmospheric river in Arizona. Part I: observed synoptic-scale, orographic, and hydrometeorological characteristics. *J Hydrometeorol* 14(2): 460–484. Retrieved Nov 24, 2021, https://journals.ametsoc.org/view/journals/hydr/14/2/jhm-d-12-0101_1.xml
- Oakley NS, Lancaster JT, Kaplan ML, Ralph FM (2017) Synoptic conditions associated with cool season post-fire debris flows in the Transverse Ranges of southern California. *Nat Hazards* 88:327–354. <https://doi.org/10.1007/s11069-017-2867-6>
- Oakley N, Cannon JF, Munroe R, Lancaster J, Gomberg D, Ralph FM (2018) Brief communication: Meteorological and climatological conditions associated with the 9 January 2018 post-fire debris flows in Montecito and Carpinteria, California, USA. *Nat Hazards Earth Syst Sci* 18:3037–3043. <https://doi.org/10.5194/nhess-18-3037-2018>
- Pierce DW, Das T, Cayan DR, Maurer EP, Miller NL, Bao Y, Kanamitsu M, Yoshimura K, Snyder MA, Sloan LC, Franco G, Tyree M (2013) Probabilistic estimates of future changes in California temperature and precipitation using statistical and dynamical downscaling. *Clim Dyn* 40:839–856
- Polade SD, Gershunov A, Cayan DR, Dettinger MD, Pierce DW (2017) Precipitation in a warming world: assessing projected hydroclimate changes in California and other Mediterranean climate regions. *Sci Rep*. <https://doi.org/10.1038/s41598-017-11285-y>
- Porter KA (2011) Overview of the ARkStorm Scenario [electronic Resource]/by Keith Porter ... [et al.]; Prepared for the U.S. Geological Survey Multihazards Demonstration Project. Reston, Va: Dept. of the Interior, U.S. Geological Survey, 2011. Print.
- Ralph FM, Neiman PJ, Wick GA (2004) Satellite and CALJET aircraft observations of atmospheric rivers over the eastern North-Pacific Ocean during the El Niño winter of 1997/98. *Mon Weather Rev* 132:1721–1745
- Ralph FM, Neiman PJ, Wick GA, Gutman SI, Dettinger MD, Cayan DR, White AB (2006) Flooding on California's Russian River: role of atmospheric rivers. *Geophys Res Lett* 33:L13801. <https://doi.org/10.1029/2006GL026689>
- Ralph FM, Neiman PJ, Kiladis GN, Weickman K, Reynolds DW (2011) A multiscale observational case study of a Pacific atmospheric river exhibiting tropical-extratropical connections and a mesoscale frontal wave. *Mon Weather Rev* 139:1169–1189. <https://doi.org/10.1175/2010MWR3596.1>
- Ralph FM, Rutz JJ, Cordeira JM, Dettinger M, Anderson M, Reynolds D, Schick LJ, Smallcomb C (2019) A scale to characterize the strength and impacts of atmospheric rivers. *Bull Am Meteorol Soc* 100(2): 269–289. Retrieved Jun 1, 2021, <https://journals.ametsoc.org/view/journals/bams/100/2/bams-d-18-0023.1.xml>
- Rhoades AM, Risser MD, Dáithí AS, Wehner MF, Jones AD (2021) Implications of warming on western United States landfalling atmospheric rivers and their flood damages. *Weather Clim Extremes* 32:100326 (ISSN 2212-0947)
- Rutz JJ, Steenburgh WJ (2012) Quantifying the role of atmospheric rivers in the interior western United States. *Atmos Sci Lett* 13:257–261. <https://doi.org/10.1002/asl.392>
- Rutz JJ, Steenburgh WJ, Ralph FM (2014) Climatological characteristics of atmospheric rivers and their inland penetration over the Western United States. *Mon Weather Rev* 142:905–921
- Rutz JJ, Steenburgh WJ, Ralph FM (2015) The inland penetration of atmospheric rivers over Western North America: a Lagrangian analysis. *Mon Weather Rev* 143(5), 1924–1944. Retrieved Aug 11, 2021. <https://journals.ametsoc.org/view/journals/mwre/143/5/mwr-d-14-00288.1.xml>
- Schwarz L, Malig BJ, Guzman Morales J, Guirguis K, Gershunov A, Basu R, Benmarhnia T (2020) The health burden of fall, winter and spring heat waves in Southern California and contribution of Santa Ana Winds. *Environ Res Lett* 15:054017
- Siirola-Woodburn E, Rhoades AM, Hatchett BJ, Huning L, Szinai J, Tague C, Nico PS, Feldman D, Jones AD, Collins WD, Kaatz L (2021) Evidence of a low-to-no snow future and its impacts on water resources in the western United States. *Nat Rev Earth Environ* 2:800–819. <https://doi.org/10.1038/s43017-021-00219-y>
- Sterle K, Hatchett BJ, Singletary L, Pohl G (2019) Hydroclimate variability in snow-fed river systems: local water managers' perspectives on adapting to the new normal. *Bull Am Meteorol Soc* 100(6):1031–1048
- Straus DM, Corti S, Molteni F (2007) Circulation regimes: chaotic variability versus SST-forced predictability. *J Clim* 20:2251–2272
- Strobin MH, Reynolds DW (1995) Forecasting hydrologically critical storms in Northern and Central California. Western Region Technical attachment 95–22, National Weather Service https://www.weather.gov/media/wrh/online_publications/TAs/ta9522.pdf. Accessed 1 Sept 2021
- Swain DL, Tsiang M, Haugen M, Singh D, Charland A, Rajaratnam B, Diffenbaugh NS (2014) The extraordinary California drought of 2013/2014: Character, context, and the role of climate change. *Bull Am Meteorol Soc* 95:S3–S7
- Swain DL, Langenbrunner B, Neelin JD et al (2018) Increasing precipitation volatility in twenty-first-century California. *Nat Clim Change* 8:427–433. <https://doi.org/10.1038/s41558-018-0140-y>
- Swales D, Alexander M, Hughes M (2016) Examining moisture pathways and extreme precipitation in the U.S. Intermountain West using self-organizing maps. *Geophys Res Lett* 43:1727–1735. <https://doi.org/10.1002/2015GL067478>
- Western Regional Climate Center (WRCC) (2021) Monthly Climate Summaries. Available online at https://wrcc.dri.edu/Climate/Monthly_Summaries/
- Uccellini LW, Ten Hoeve JE (2019) Evolving the National Weather Service to Build a Weather-Ready Nation: connecting observations, forecasts, and warnings to decision-makers through impact-based decision support services. *Bull Am Meteorol Soc* 100(10):

- 1923–1942. Retrieved Aug 30, 2021, <https://journals.ametsoc.org/view/journals/bams/100/10/bams-d-18-0159.1.xml>
- Vahedifard F, Aghakouchak A, Ragno E, Shahrokhbadi S, Malakpour I (2017) 2017: lessons from the Oroville dam. *Science* 17:1139–1140
- Weaver R (1962) Meteorology of hydrologically Critical Storms in California. Hydrometeorological Report No. 37, U.S. Dept. of Commerce, Weather Bureau (now the National Weather Service) <https://cepsym.org/history/HMR-37.pdf>. Accessed 1 Sept 2021
- Westerling AL, Cayan DR, Brown TJ, Hall BL, Riddle LG (2004) Climate, Santa Ana winds and autumn wildfires in southern California. *Eos Trans Amer Geophys Union* 85:289–296. <https://doi.org/10.1029/2004EO310001>
- Zhang Z, Ralph FM, Zheng M (2019) The relationship between extratropical cyclone strength and atmospheric river intensity and position. *Geophys Res Lett* 46:1814–1823. <https://doi.org/10.1029/2018GL079071>

Publisher's Note Springer Nature remains neutral with regard to jurisdictional claims in published maps and institutional affiliations.